



WARNING TIMES AND IMPACT PREDICTIONS
OF ASTEROIDS AND COMETS ON A COLLISION
COURSE WITH EARTH

THESIS

Ahren D. Heidt, Captain, USAF

AFIT/GSO/ENY/97D-1

DISTRIBUTION STATEMENT A

Approved for public release
Distribution Unlimited

DEPARTMENT OF THE AIR FORCE
AIR UNIVERSITY
AIR FORCE INSTITUTE OF TECHNOLOGY

Wright-Patterson Air Force Base, Ohio

DTIC QUALITY INSPECTED 8

19980121 061

AFIT/GSO/ENY/97D-1

WARNING TIMES AND IMPACT PREDICTIONS
OF ASTEROIDS AND COMETS ON A COLLISION
COURSE WITH EARTH

THESIS

Ahren D. Heidt, Captain, USAF

AFIT/GSO/ENY/97D-1

Approved for public release; distribution unlimited

DTIC QUALITY INSPECTED 3

The views expressed in this thesis are those of the author and do not reflect the official policy or position of the Department of Defense or the U. S. Government.

WARNING TIMES AND IMPACT PREDICTIONS
OF ASTEROIDS AND COMETS ON A COLLISION
COURSE WITH EARTH

THESIS

Presented to the Faculty of the Graduate School of Engineering
of the Air Force Institute of Technology

Air University

Air Education and Training Command

In Partial Fulfillment of the Requirements for the
Degree of Master of Science in Space Operations

Ahren D. Heidt, B.S.

Captain, USAF

December 1997

Approved for public release; distribution unlimited

WARNING TIMES AND IMPACT PREDICTIONS
OF ASTEROIDS AND COMETS ON A COLLISION
COURSE WITH EARTH

Ahren D. Heidt, B.S.
Captain, USAF

Approved:

William E. Wiesel

Dr. William E. Wiesel (Chairman)

26 Nov 97

date

Sharon E. Heise

Captain Sharon Heise

26 Nov 97

date

Bradley S. Liebst

Dr. Bradley S. Liebst

26 Nov 97

date

Acknowledgments

I would like to thank Dr. William E. Wiesel, who provided guidance along the way when I needed it, but let go of the reins when I didn't. I would also like to thank my wife Nicole Marie who has not only supported me through it all, but did so while carrying our second child, during the hot, humid summer, with a second-hand air conditioner and our first child at her heels (uphill both ways). Jadon was born on 17 Oct 97, much to the chagrin of his older brother Kaleb. My family deserves all the credit in the world for their understanding and patience. I'd write more, but they're waiting for me in the car. We're headed for Disneyland.

Ahren D. Heidt

Table of Contents

	Page
Acknowledgements	iii
List of Figures	vii
List of Tables.....	xi
Abstract.....	xii
I. INTRODUCTION	1-1
1.1 Background.....	1-1
1.2 Problem	1-2
1.3 Research Objective	1-2
1.4 Thesis Overview	1-3
II. LITERATURE REVIEW.....	2-1
2.1 Introduction	2-1
2.2 Origin of Comets and Asteroids	2-1
2.3 Physical Properties.....	2-2
2.4 The Threat from Comets and Asteroids.....	2-3
2.4.1 Speed and Density.....	2-5
2.5 Search Techniques	2-6
2.5.1 Photographic Techniques	2-6
2.5.2 Charge-Coupled Device Techniques	2-7
2.5.3 Dedicated NEO Search Programs.....	2-7
2.6 Impact Prediction.....	2-8
2.7 Hazard Mitigation.....	2-10
III. METHODOLOGY	3-1
3.1 The N-body Problem.....	3-1
3.1.1 Equations of Motion.....	3-1
3.2 FORTRAN Program Library.....	3-4
3.3 Impact Conditions.....	3-6
3.4 Integrating the Trajectory.....	3-8
3.5 Creating Observation Data.....	3-9
3.6 The Bayes Filter.....	3-10
3.7 Impact Prediction.....	3-12

IV. RESULTS AND ANALYSIS	4-1
4.1 The Extreme Trajectories	4-1
4.1.1 Trajectory 1.....	4-2
4.1.2 Trajectory 2.....	4-4
4.1.3 Trajectory 3.....	4-6
4.1.4 Trajectory 4.....	4-8
4.1.5 Trajectory 5.....	4-10
4.1.6 Trajectory 6.....	4-12
4.1.7 Trajectory 7.....	4-14
4.2 Sensitivity Analysis	4-15
4.2.1 Trajectory 8.....	4-16
4.2.1.1 100 Observations Per Day	4-18
4.2.1.2 1000 Observations Per Day.....	4-19
4.2.1.3 1.0 Arcsecond Accuracy	4-20
4.2.1.4 0.01 Arcsecond Accuracy	4-21
4.2.1.5 Observations from 2 Sites Rotating on the Surface of the Earth	4-21
4.2.1.6 Observations from Geosynchronous Orbit	4-22
4.2.1.7 Observations from the Moon	4-23
4.2.1.8 Observations from Mars	4-24
4.2.1.9 Range, Azimuth, and Elevation Observations from Earth.....	4-25
4.2.1.10 Observations from Earth and Geosynchronous Orbit.....	4-26
4.2.1.11 Observations from Earth and the Moon.....	4-27
4.2.1.12 Observations from Earth and Mars.....	4-28
4.2.1.13 Observations from Earth and an Out of Plane Orbit	4-29
4.2.2 Trajectory 9.....	4-30
4.2.2.1 100 Observations Per Day	4-32
4.2.2.2 1000 Observations Per Day.....	4-33
4.2.2.3 1.0 Arcsecond Accuracy	4-34
4.2.2.4 0.01 Arcsecond Accuracy	4-35
4.2.2.5 Observations from the Moon	4-36
4.2.2.6 Observations from Earth and the Moon.....	4-37
4.2.2.7 Observations from Earth and Mars.....	4-38
4.2.2.8 Observations from Earth and an Out of Plane Orbit	4-39
4.2.3 Trajectory 1 (Revisited).....	4-40
4.2.3.1 100 Observations Per Day	4-42
4.2.3.2 1000 Observations Per Day.....	4-43
4.2.3.3 1.0 Arcsecond Accuracy	4-44
4.2.3.4 0.01 Arcsecond Accuracy	4-45
4.2.3.5 Observations from the Moon	4-46
4.2.3.6 Observations from Earth and the Moon.....	4-47
4.2.3.7 Observations from Earth and Mars.....	4-48
4.2.3.8 Observations from Earth and an Out of Plane Orbit	4-49

V. CONCLUSIONS AND RECOMMENDATIONS	5-1
5.1 Conclusions	5-1
5.2 Recommendations.....	5-2
Bibliography.....	BIB-1
Vita	VITA-1

List of Figures

Figure	Page
3.1. Final Impact Conditions.....	3-6
3.2. Terrestrial Impact Speeds for Observed Long Period Comets.....	3-7
3.3. Error Ellipsoid in the XYZ-Frame.....	3-12
3.4. Error Ellipsoid in the E-Frame	3-14
4.1. Trajectory 1 (Overhead View)	4-2
4.2. Error Ellipsoid (Velocity In, North Up).....	4-3
4.3. Error Ellipsoid (Velocity Up, North Out)	4-3
4.4. Trajectory 2 (Overhead View)	4-4
4.5. Error Ellipsoid (Velocity In, North Up).....	4-5
4.6. Error Ellipsoid (Velocity Up, North Out)	4-5
4.7. Trajectory 3 (Overhead View)	4-6
4.8. Error Ellipsoid (Velocity In, North Up).....	4-7
4.9. Error Ellipsoid (Velocity Up, North Out)	4-7
4.10. Trajectory 4 (Overhead View).....	4-8
4.11. Error Ellipsoid (Velocity In, North Up).....	4-9
4.12. Error Ellipsoid (Velocity Up, North Out)	4-9
4.13. Trajectory 5 (Overhead View).....	4-10
4.14. Error Ellipsoid (Velocity In, North Up).....	4-11
4.15. Error Ellipsoid (Velocity Up, North Out)	4-11
4.16. Trajectory 6 (Overhead View).....	4-12
4.17. Error Ellipsoid (Velocity In, North Up).....	4-13

4.18. Error Ellipsoid (Velocity Up, North Out)	4-13
4.19. Trajectory 7 (Overhead View).....	4-14
4.20. Error Ellipsoid (Velocity In, North Up).....	4-15
4.21. Error Ellipsoid (Velocity Up, North Out)	4-15
4.22. Trajectory 8 (Overhead View).....	4-16
4.23. Error Ellipsoid (Velocity In, North Up).....	4-17
4.24. Error Ellipsoid (Velocity Up, North Out)	4-17
4.25. Error Ellipsoid (Velocity In, North Up).....	4-18
4.26. Error Ellipsoid (Velocity Up, North Out)	4-18
4.27. Error Ellipsoid (Velocity In, North Up).....	4-19
4.28. Error Ellipsoid (Velocity Up, North Out)	4-19
4.29. Error Ellipsoid (Velocity In, North Up).....	4-20
4.30. Error Ellipsoid (Velocity Up, North Out)	4-20
4.31. Error Ellipsoid (Velocity In, North Up).....	4-21
4.32. Error Ellipsoid (Velocity Up, North Out)	4-21
4.33. Error Ellipsoid (Velocity In, North Up).....	4-22
4.34. Error Ellipsoid (Velocity Up, North Out)	4-22
4.35. Error Ellipsoid (Velocity In, North Up).....	4-23
4.36. Error Ellipsoid (Velocity Up, North Out)	4-23
4.37. Error Ellipsoid (Velocity In, North Up).....	4-24
4.38. Error Ellipsoid (Velocity Up, North Out)	4-24
4.39. Error Ellipsoid (Velocity In, North Up).....	4-25
4.40. Error Ellipsoid (Velocity Up, North Out)	4-25

4.41. Error Ellipsoid (Velocity In, North Up).....	4-26
4.42. Error Ellipsoid (Velocity Up, North Out)	4-26
4.43. Error Ellipsoid (Velocity In, North Up).....	4-27
4.44. Error Ellipsoid (Velocity Up, North Out)	4-27
4.45. Error Ellipsoid (Velocity In, North Up).....	4-28
4.46. Error Ellipsoid (Velocity Up, North Out)	4-28
4.47. Error Ellipsoid (Velocity In, North Up).....	4-29
4.48. Error Ellipsoid (Velocity Up, North Out)	4-29
4.49. Trajectory 9 (Overhead View).....	4-30
4.50. Error Ellipsoid (Velocity In, North Up).....	4-31
4.51. Error Ellipsoid (Velocity Up, North Out)	4-31
4.52. Error Ellipsoid (Velocity In, North Up).....	4-32
4.53. Error Ellipsoid (Velocity Up, North Out)	4-32
4.54. Error Ellipsoid (Velocity In, North Up).....	4-33
4.55. Error Ellipsoid (Velocity Up, North Out)	4-33
4.56. Error Ellipsoid (Velocity In, North Up).....	4-34
4.57. Error Ellipsoid (Velocity Up, North Out)	4-34
4.58. Error Ellipsoid (Velocity In, North Up).....	4-35
4.59. Error Ellipsoid (Velocity Up, North Out)	4-35
4.60. Error Ellipsoid (Velocity In, North Up).....	4-36
4.61. Error Ellipsoid (Velocity Up, North Out)	4-36
4.62. Error Ellipsoid (Velocity In, North Up).....	4-37
4.63. Error Ellipsoid (Velocity Up, North Out)	4-37

4.64. Error Ellipsoid (Velocity In, North Up).....	4-38
4.65. Error Ellipsoid (Velocity Up, North Out)	4-38
4.66. Error Ellipsoid (Velocity In, North Up).....	4-39
4.67. Error Ellipsoid (Velocity Up, North Out)	4-39
4.68. Trajectory 1 (Overhead View).....	4-40
4.69. Error Ellipsoid (Velocity In, North Up).....	4-41
4.70. Error Ellipsoid (Velocity Up, North Out)	4-41
4.71. Error Ellipsoid (Velocity In, North Up).....	4-42
4.72. Error Ellipsoid (Velocity Up, North Out)	4-42
4.73. Error Ellipsoid (Velocity In, North Up).....	4-43
4.74. Error Ellipsoid (Velocity Up, North Out)	4-43
4.75. Error Ellipsoid (Velocity In, North Up).....	4-44
4.76. Error Ellipsoid (Velocity Up, North Out)	4-44
4.77. Error Ellipsoid (Velocity In, North Up).....	4-45
4.78. Error Ellipsoid (Velocity Up, North Out)	4-45
4.79. Error Ellipsoid (Velocity In, North Up).....	4-46
4.80. Error Ellipsoid (Velocity Up, North Out)	4-46
4.81. Error Ellipsoid (Velocity In, North Up).....	4-47
4.82. Error Ellipsoid (Velocity Up, North Out)	4-47
4.83. Error Ellipsoid (Velocity In, North Up).....	4-48
4.84. Error Ellipsoid (Velocity Up, North Out)	4-48
4.85. Error Ellipsoid (Velocity In, North Up).....	4-49
4.86. Error Ellipsoid (Velocity Up, North Out)	4-49

List of Tables

Table	Page
2.1. NEO Threat Groups.....	2-4
2.2. Range Limits for Radar Astrometry of New NEOs	2-9

Abstract

This study investigates the amount of data and time necessary to accurately predict Earth impacts of Earth-Crossing-Objects (ECOs). Trajectories are simulated by numerically integrating in an N-Body system. Given final impact parameters, the trajectory is propagated backwards to an earlier time, creating initial conditions and simulated observation data at requested intervals to which Gaussian random noise is introduced. Utilizing a Bayes Filter to estimate position and velocity from the simulated observation data, the estimate is then propagated forward in time to determine whether or not an impact can be accurately predicted. State vectors and covariance matrices are then propagated to the impact time and the one-sigma error ellipsoid is analyzed.

**WARNING TIMES AND IMPACT PREDICTIONS
OF ASTEROIDS AND COMETS ON A COLLISION
COURSE WITH EARTH**

I. Introduction

1.1 Background

“In the year 1999 and seven months the Great King of Terror will come from the sky, he will bring back to life the great king of the Mongols. Before and after the God of war reigns happily (11:34).” The preceding quote, by Nostradamus, has been interpreted by some to predict the impact of a comet or asteroid with the Earth.

In the last twenty years, the importance of large impacts for the origin and evolution of life on Earth has become increasingly apparent. It is now widely accepted that the impact of a 10-km diameter asteroid or comet caused the extinction of the dinosaurs and of a multitude of other life forms 65 million years ago. (5:711)

Recently, the publicity surrounding possible impacts of asteroids and comets with the Earth has grown tremendously with books as well as movies describing various scenarios and outcomes.

Near-Earth-Objects (NEOs) are asteroids and comets whose orbits cross the orbit of the Earth (8:1). Although the daily or annual probabilities of NEO collisions with the Earth are infinitesimal, the expected value of the casualties and damage that could result from one is catastrophic. A fast and reliable system needs to be put in place to detect,

track and deter an incoming object. The fact is that a threat does exist, the next step is to decide what measures to take to deal with that threat.

1.2 Problem

The problem is that once an NEO is detected, it must be tracked to determine if it will impact with the Earth. If it is found to be on an intercept course with the Earth, and if it is large enough and dense enough to pose a threat to the Earth, then an attempt must be made to deflect it. That is, of course, if there is enough time to accomplish such a task.

Therefore, once an NEO is detected, it is imperative to gather as much data as is feasible and once the trajectory is determined to pass near the Earth, the trajectory must be quickly and accurately determined. A system must be in place if and when this happens to obtain the type and accuracy of observations needed to accomplish this task.

1.3 Research Objective

The objective of this research is to determine how quickly it can be determined whether or not an NEO will impact with the Earth. The research encompasses both asteroids and comets, however, the initial detection of the NEOs is assumed to occur at a distance of 3 AU from the sun, which displays more emphasis on comets. This is due to the fact that comets "turn on" at this distance from the sun.

Various observational systems will be analyzed and compared to illustrate what methods are most useful for accurately determining trajectories and future impacts.

1.4 Thesis Overview

This thesis contains four specific areas of interest. These include:

- Asteroid and Comet Background and Investigation
- Search Techniques, Impact Prediction, and Hazard Mitigation
- Model Development
- Analysis of Results

II. Literature Review

2.1 Introduction

This chapter provides a broad, general sphere of information that encompasses information relevant to the development of this thesis. This literature review was written with the goal of creating a basis for further research. This review will cover the following topics:

- Origin of Comets and Asteroids
- Physical Properties
- The Threat from Comets and Asteroids
- Search Techniques
- Impact Prediction
- Hazard Mitigation

2.2 Origin of Comets and Asteroids

Approximately four and a half billion years ago, the solar system formed through the coagulation of gas and dust. Initially, collections of rocky materials formed, which in turn merged together to create planets. As the planets formed, they slowly absorbed the loose material still orbiting through the solar system. Focusing on Earth, the bombardment began to slow, leading to the cooling of the planet and solidification of the Earth's crust. At this time, however, no water existed on Earth. Comets arriving from

the outer edges of the solar system brought the water that now covers three quarters of the Earth's surface. Life began evolving soon after (9:54).

The vast majority of asteroids lie in a large belt between the orbits of Mars and Jupiter. Due to their proximity to the sun, temperatures were relatively hot during their formation. These high temperatures vaporized the lighter substances such as water, leaving mostly silica, carbon, and metals (9:54).

Comets, unlike asteroids, began as material flung beyond the orbit of Neptune during the solar system's formation. At this distance from the sun, the temperature is approximately -260 degrees Celsius in space. Due to these temperatures, comets retained their volatile materials, such as gas, ice, and snow, during formation. Comets usually contain loosely packed carbon and other light elements (9:54).

2.3 Physical Properties

In researching asteroid and comet composition, an infinite number of possible groupings exist. For the purposes of ranking them, however, NEO materials will be divided into three groups.

The first group is NEO material 0 and contains NEOs characterized as extinct comet nuclei. These objects tend to have a very low density of 0.2 to 1.5 g/cm³. Other properties include poor mechanical strength, variable refractory organic materials, ice, some iron, and manganese. Variable refractory organic materials include carbon, hydrogen, nitrogen, and oxygen. Typical variations include varied nuclear radiation absorption dependent upon selective molecular and atomic losses, in addition to random structural integrity depending on the structure of individual comets (15:589).

NEO material 1 is related to the structurally weakest asteroids. These objects have low density, low conductivity, a high melting point, and a low albedo. Typical elements present include silicon, oxygen, iron, manganese, and sulfur. In addition, X-ray absorption is much higher than in NEO material 0. Low crushing strengths and low structural integrity are results of porosity and faults (15:589).

NEO material 2 lies in between NEO material 1 and NEO material 3 with respect to structural strength and integrity. Concerning materials, material 2 is richer in silicon, iron, and manganese than material 1. The thermal properties of material 2 are similar to those of material 1. Characteristics of material 2 include higher density, conductivity, melting point, albedo, and X-ray absorption than material 1. Material 2 also has less porosity and a higher crushing strength (15:589).

NEO material 3 is the strongest group and resembles stainless steel to some extent. These asteroids have very high density and virtually no porosity resulting in the strongest mechanical structure. For similar reasons, material 3 also possesses the most uniform thermal characteristics. Electrical conductivity, thermal conductivity, and X-ray absorption are all extremely high (15:590).

2.4 The Threat from Comets and Asteroids

In 1981, researchers discovered that a thin, global sediment layer that separates the end of the Cretaceous era (the last period of the age of dinosaurs) from the beginning of the Tertiary era (the start of the age of mammals) contained the unmistakable signature of an asteroid or comet impact. (12:16)

The current population estimate of NEOs includes 2000 asteroids larger than one kilometer and 300,000 asteroids larger than 100 meters in diameter (8:1). In an attempt

to characterize and quantify the threat, the NEO threat has been divided into four arbitrary groups as shown in Table 2.1.

Table 2.1. NEO Threat Groups (1:4)

	Impact Frequency (years)	Impact Energy (MT of TNT)	Impactor Diameter (meters)	Example of Occurrence	Relevance to Mankind
Destroyed in the Upper Atmosphere	Group I		10 to 1000 (*10 ⁴ Objects)		
	1	0.02	10	Annual Event occurring over unpopulated areas	Size of the A Bomb that ended WW II
	Group II		10 ⁴ Objects		
Most Probable Occurrence	10	0.2	20-30	Occasional Event occurring over unpopulated areas	Large A Bomb Size
Most Difficult to Detect	(30)	0.7-1.0		1931 Incident at Curuca?	<i>Surprise Event</i>
Non-nuclear Mitigation	100	12-15	50-90 (25-33) iron	1908 Tunguska Meteor Crater Arizona	Size of H Bomb (<i>Destroys Cities-e.g. L.A.</i>)
2-4 Mill. Deaths	Group III		10 ³ Objects		
	1,000	50	100-200	Lunar Crater & <i>Alleged Biblical Event</i>	Largest H Bomb By Soviets was 58 Megatons
	10,000	1000	500 (430-2300)	Lunar Craters Asteroid 1989 FC (undetected near miss)	Major Global Effects <i>Surprise Event</i>
Transition	Group IV		1000 to 2000 Objects		
	1,000,000	1,000,000	1 Km.	Lunar Craters	Certain Global Catastrophe
	10,000,000	1*10 ⁷ +	2 Km.	Lunar Craters (e.g. <i>Aristillus</i>)	
Least Probable Occurrences	Uncertain	20*10 ⁷ +	10 Km.	Impact Extinction of Dinosaurs Shoemaker-Levy-9	Thousand Times Stronger Than World's Arsenal of Nuclear Weapons
Easiest to Detect					
Nuclear Mitigation					
40 Mill.+ Deaths					
Mass Extinctions					

Group I consists of small objects with diameters on the order of 10 meters that would likely burn up in the upper atmosphere. A group I object enters the Earth's atmosphere once a year, on average. The energy release during this event is approximately 20,000

tons of TNT, which is roughly equivalent to the atomic bombs that ended World War II (1:4).

Group II is comprised of 20 to 30 meter diameter objects, which may be of concern, depending on composition and velocity. Typically, a group II object impacts the Earth every 10 to 100 years. The object has a good chance of reaching the Earth's surface depending on size and density. A group II impact can release anywhere from 0.2 to 15 MT of TNT, which is enough to destroy an entire city. This is a likely occurrence, since the size of these objects makes them very hard to detect, and the timeline makes them more likely than the larger threats (1:4).

Topping out at 1 kilometer in diameter, Group III objects represent threats that could have major global environmental effects and regional catastrophes. The timeline for a group III impact is on the order of 1,000 to 10,000 years (1:4).

Even more so are Group IV objects, 1 kilometer and larger, which would produce global catastrophic events, the most severe of which are mass extinctions. These events are predicted to occur every 1 million to 10 million years (1:4). Although a major impact is unlikely, the severity of such an occurrence to our fragile society demands that we prepare adequately for such a scenario. If it is possible to predict such an event, it stands to reason that the world as a whole would make every effort to deter it.

2.4.1 Speed and Density. The threat of asteroids and comets are often categorized according to size for simplicity sake, however, several other factors are involved in determining the actual results of an impact. Some of these include speed, density, and direction of impact.

The density of objects larger than 1 kilometer makes essentially no difference. For impactors of this size, Earth's atmosphere is thin and the ultimate damage is proportional to the kinetic energy of the object and any fragments that break off the object (7:546). It is the total mass that determines the actual kinetic energy possessed by the object, not the density.

For the same reason, speed plays a large role in determining possible affects of an impact. As seen in the equation:

$$KE = \frac{1}{2}mv^2 \quad (2-1)$$

kinetic energy is proportional to the square of the velocity.

2.5 Search Techniques

Prior to the 1970s, NEOs were detected purely by chance. In fact, NEOs typically just annoyed astronomers, who threw away the photographs that they considered to be ruined by the foreign objects. Post 1970, discoveries were made by comparing two photographic plates taken during a particular interval of time. The principle is that objects appear to move at a slower angular rate when they are far away, and at a faster rate when they are closer (10:2). Present day techniques include two primary categories.

2.5.1 Photographic Techniques. Various photographic techniques exist in which to detect and track NEOs, but the common goal of all photographic techniques is prompt follow-up after the initial exposure (6:136). Angular motions of NEOs are typically on the order of 1 degree per day. This combined with initial directional ambiguity results in an object that is easily lost if not promptly reacquired.

Long exposures provide a better means of picking out NEOs from the background on which they are photographed. This is due to the fact that with long exposures, moving objects leave a tail that is more easily identified. At the same time, stars are easily filtered out.

One fairly new method involves the use of stereo comparators to examine pairs of photographs of the same part of the sky. The two images are transformed into one by looking at one photograph with each eye. Due to a physiological effect, the image will appear to stand above or below the plane of the photograph if it is moving (6:136).

2.5.2 Charge-Coupled Device Techniques. Charge-Coupled Devices (CCDs) revolutionized the ability to search for asteroids and comets. The CCDs use photo detectors similar to those found in the average Video Camera, which trap photons and convert them to electrons. As a result, the labor-intensive task of studying photographs became a software-based task. Two distinct observational techniques are used by CCDs, staring and scanning (6:136). The technique of staring simply involves the telescope viewing one location and detecting any movement. The scanning technique involves moving the telescope or fixing it in place as the Earth rotates and looking for moving objects.

2.5.3 Dedicated NEO Search Programs. Four programs have existed for an extended period of time, which continuously monitor the skies in an effort to detect NEOs. These are the Palomar Planet-Crossing Asteroid Survey, the Palomar Asteroid and Comet Survey, the Spacewatch Program, and Anglo-Australian Near-Earth Asteroid Survey, which is the only program located in the Southern Hemisphere. The Spacewatch Program is primarily a developmental program, aimed at developing new techniques to

improve discovery rates (10:3). Added to this, amateur astronomers also contribute to the number of detected NEOs.

Additional programs which are currently coming on-line include the Near-Earth Asteroid Tracking program which uses a CCD and a GEODSS Telescope, the Observatoire de la Cote d'Azur, which will use a similar system, and the Lowell Observatory Near-Earth Object Survey, which does not use a CCD, but intends to compare photographs with existing star catalogues to identify objects (10:3).

The combined efforts of these programs strive to discover about 90 percent of the one-kilometer asteroids by 2010. Comets, on the other hand, tend to have very long periods with nearly parabolic orbits. They can be kicked out of the Oort cloud or the Kuiper Belt and run straight into the Earth without any previous observational history. Comet detection will never be complete, and a continuous search effort must be sustained (10:3).

2.6 Impact Prediction

At best, very limited literature exists concerning impact prediction. Even less exists with respect to timely impact prediction. Timely impact predictions refer to those NEOs which are detected two to three months before impact, and it must be determined whether immediate action must be taken.

The typical scenario involved asteroids that have been discovered and tracked for an extended period of time. When an adequate amount of data is accumulated, an impact is predicted several years and orbits away and people must sit down and come up with a

plan to deflect the asteroid. For these types of situations, data accuracy is not necessarily imperative since enough data will accumulate over time to counter any inaccuracies.

The more immediate threat comes from comets or asteroids that are discovered a short time before impact on their final leg. It takes several observations just to determine if the object is headed in the general direction of the Earth. Once that is done, present techniques require a large amount of data to accurately determine a future impact. The possibility exists for a NEO that would initially barely miss the Earth on the order of one to several Earth radii, to be fragmented by a deflection device, causing damage which otherwise would have been avoided.

Presently, two types of observations are taken, optical and radar. For optical observations, telescopes are used to determine an object's azimuth and elevation angles. These angles are typically fairly accurate. However, there is essentially no range information derived. This poses a large problem when NEOs are headed straight for the Earth and, observationally, they appear to remain stationary in the sky.

Radar observations can be acquired with present day technology, but only for close-approach objects. Arecibo and Goldstone are the primary NEO radar observatories. Table 2.2 summarizes their respective ranges for various sizes of objects corresponding to a relatively low signal-to-noise ratio.

Table 2.2. Range Limits for Radar Astrometry of New NEOs (14:274)

Diameter	Arecibo	Goldstone
10 m	0.042 AU	0.018 AU
100 m	0.10 AU	0.042 AU
1 km	0.24 AU	0.10 AU
10 km	0.56 AU	0.24 AU

Future advances include the development of longer ranged radar and lasers that can accomplish the same task as radar, but with accuracies down to the centimeter level. With advances in technology, accuracies will also increase and the number of observations that can be taken in a given period of time may increase.

Other possibilities include the placement of observation instruments at locations other than the Earth. These instruments can be placed on satellites and launched into various orbits or placed on another planet or moon.

2.7 Hazard Mitigation

Three primary mitigation techniques exist for a situation in which it is determined that an object will hit the Earth. These are passive measures, non-destructive counterforce, and threat termination (2:10).

The first technique can involve evacuations and some logistics efforts if the location of the future impact is known accurately, especially if it is in the proximity of large populations (2:10). The passive measures are fine for small impactors that will not cause residual effects, however, they are not acceptable for objects larger than one kilometer.

The second technique is using a non-destructive counterforce to alter the NEO's trajectory enough to miss the Earth. An example of this method is the use of a nuclear warhead detonated above the surface of the NEO to propel it in a given direction without destroying it. Solar sails may also be attached to an object to slowly alter the trajectory using the solar wind as propulsion (2:10).

Threat termination involves the total destruction of a body. This can be accomplished by nuclear weapons detonated beneath the surface or with high speed impacting devices. There is uncertainty in determining what will happen to the object fragments. Even if the fragments are blown apart, if they all still hit the Earth, the total energy released remains the same as if they were still one body. If this technique is used, it must be accomplished in such a way as to prevent such an outcome.

III. Methodology

3.1 The N-body Problem

The n-body problem is used to describe the motion of a body (in our case a comet or asteroid) which is acted upon by other gravitational masses and possible other forces such as drag, thrust and solar radiation pressure (3:5). The entire system is made up of n-bodies ($m_1, m_2, m_3 \dots m_n$) and the body we wish to study is contained within it. This is the i^{th} body, m_i . In order to determine the equations of motion, the vector sum of all gravitational forces and other external forces acting on m_i will be used. Making the assumption that the planets are spherical, Newton's law of universal gravitation can be applied to determine the gravitational forces.

3.1.1 Equations of Motion. For simplicity, I have chosen a coordinate system centered at the sun, with the x-axis in the direction of Aries, and the z-axis perpendicular to the plane of the Earth's orbit (towards Polaris). The following derivation of the resulting equations of motion for this coordinate system can be found in Fundamentals of Astrodynamics by Bate, Mueller, and White, pages 7-10. Knowing the classical orbital elements of all of the planets, by picking a particular time, the positions of all the planets can be found $\vec{r}_1, \vec{r}_2, \vec{r}_3 \dots \vec{r}_n$.

If Newton's law of universal gravitation is applied, the force \vec{F} exerted on m_i by m_n is:

$$\vec{F}_{gn} = -\frac{Gm_i m_n}{r_{ni}^3}(\vec{r}_{ni}) \quad (3-1)$$

where

$$\vec{r}_{ni} = \vec{r}_i - \vec{r}_n \quad (3-2)$$

The vector sum of all gravitational forces acting on the i^{th} body, simplified with summation notation, may be written as:

$$\vec{F}_g = -Gm_i \sum_{j=1, j \neq i}^n \frac{m_j}{r_{ji}^3}(\vec{r}_{ji}) \quad (3-3)$$

The $j \neq i$ in the summation notation accounts for the fact that the i^{th} object does not exert a force on itself.

Although external forces are not taken into account for this thesis, at this point any other external forces, \vec{F}_{OTHER} , including drag, thrust, solar radiation pressure, perturbations due to nonspherical shapes, etc., are added. The combined force acting on the i^{th} body is \vec{F}_{TOTAL} .

$$\vec{F}_{TOTAL} = \vec{F}_g + \vec{F}_{OTHER} \quad (3-4)$$

Applying Newton's second law of motion:

$$\frac{d}{dt}(m_i \vec{v}_i) = \vec{F}_{TOTAL} \quad (3-5)$$

Taking the time derivative and assuming m_i is constant:

$$m_i \frac{d\vec{v}_i}{dt} = \vec{F}_{TOTAL} \quad (3-6)$$

and dividing through by mass m_i gives the most general equation:

$$\ddot{\vec{r}}_i = \frac{\vec{F}_{TOTAL}}{m_i} \quad (3-7)$$

where

$\ddot{\vec{r}}_i$ is the vector acceleration of the i^{th} body

m_i is the mass of the i^{th} body

Assuming that the mass of the i^{th} body remains constant, and that drag and other external forces are not present, the only forces left are gravitational. The resultant equation is then:

$$\ddot{\vec{r}}_i = -G \sum_{j=1, j \neq i}^n \frac{m_j}{r_{ji}^3} (\vec{r}_{ji}) \quad (3-8)$$

Now assume that m_2 is an NEO and that m_1 is the sun. The remaining masses $m_3, m_4 \dots m_n$ may be the Earth and other planets. From equation 3-2 it is apparent that:

$$\vec{r}_{12} = \vec{r}_2 - \vec{r}_1 \quad (3-9)$$

and

$$\ddot{\vec{r}}_{12} = \ddot{\vec{r}}_2 - \ddot{\vec{r}}_1 \quad (3-10)$$

Combining this with equation 3-8 gives:

$$\ddot{\vec{r}}_{12} = -G \sum_{j=1, j \neq 2}^n \frac{m_j}{r_{j2}^3} (\vec{r}_{j2}) + G \sum_{j=2}^n \frac{m_j}{r_{j1}^3} (\vec{r}_{j1}) \quad (3-11)$$

Since $\vec{r}_{12} = -\vec{r}_{21}$ the first terms in each bracket may be combined, resulting in:

$$\ddot{\vec{r}}_{12} = -\frac{G(m_1 + m_2)}{r_{12}^3} (\vec{r}_{12}) - \sum_{j=3}^n Gm_j \left(\frac{\vec{r}_{j2}}{r_{j2}^3} - \frac{\vec{r}_{j1}}{r_{j1}^3} \right) \quad (3-12)$$

$\ddot{\vec{r}}_{12}$ is the acceleration of the NEO relative to the sun. The last term in equation 3-12 accounts for the perturbing effects of the Earth and other planets.

3.2 FORTRAN Program Library.

Dr. William E. Wiesel created several Fortran subroutines that my thesis relied heavily upon (17). Dr. Wiesel additionally provided information and guidance concerning additions and alterations made to this code. A large number of additional modifications were made, however, many modifications and subroutines created for this thesis are based upon original code developed by Dr. Wiesel.

Fortran subroutines created by Dr. Wiesel:

- Subroutine Moveit. Uses initial conditions to move object forward in time
- Subroutine Haming. Ordinary differential equations integrator supplied (not created) by Dr. Wiesel.
- Subroutine Rhs. Calculates the state transition matrix.
- Subroutine Bayes. Simulates a Bayes Filter, which is an estimation algorithm.
- Subroutine Obser. Calculates angles only observations.
- Function Randg. Gaussian pseudo random number generator.
- Subroutine Julday. Converts date and time information to modified Julian day.
- Subroutine Phpph. Propagates the covariance matrix.
- Subroutine Fotbal. Performs Gaussian elimination with maximal pivoting.
- Subroutine Eigrf. IMSL-like eigenvalue routine.
- Subroutine Eigen. Generates eigenvalues of a real general matrix.
- Subroutine Compve. Finds complex eigenvectors corresponding to complex eigenvalues.
- Subroutine Hesqr. Finds all eigenvalues of a real general matrix.

- Subroutine Reolve. Calculates real eigenvectors of a matrix in upper heisenberg form.
- Subroutine Escale. Scales a matrix and normalizes.

The Netlib repository contains freely available software, documents, and databases of interest to the numerical, scientific computing, and other communities. The repository is maintained by AT&TBell Laboratories, the University of Tennessee and Oak Ridge National Laboratory, and by colleagues worldwide.

Fortran subroutines found in the Netlib repository:

- Subroutine Dgedi. Computes the determinant and inverse of a matrix using the pivot vector from Dgefa.
- Subroutine Dgefa. Factors a double precision matrix by Gaussian elimination and creates an integer vector of pivot indices.

Fortran Subroutines created during this thesis:

- Subroutine Check. After each block of data is processed by the bayes subroutine, check determines whether or not the object will impact the earth taking into account the positional error ellipsoids.
- Subroutine Transfers. Modified form of Moveit. Uses impact conditions provided by the user to propagate backwards in time, in order to determine the object's initial conditions at a distance of 3 AU away from the sun. Then uses initial conditions to create simulated data for Bayes Filter.

3.3 Impact Conditions

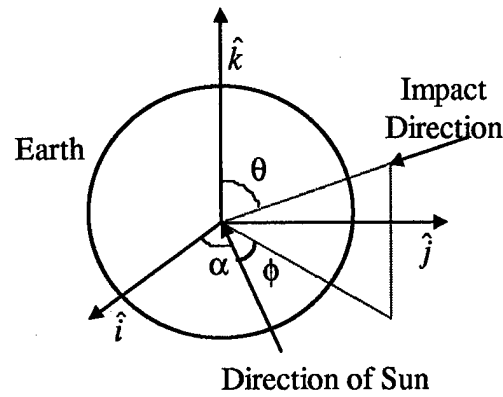


Figure 3.1. Final Impact Conditions

Given the parameters shown in the above figure, the position (in the xyz-frame) at impact on the surface of the Earth is:

$$x = x_{earth} + R_{earth} \cos(\alpha + \phi) \sin(\theta) \quad (3-13)$$

$$y = y_{earth} + R_{earth} \sin(\alpha + \phi) \sin(\theta) \quad (3-14)$$

$$z = R_{earth} \cos(\theta) \quad (3-15)$$

where x_{earth} , y_{earth} , and z_{earth} are the coordinates of the Earth in the xyz-frame, and R_{earth} is the radius of the Earth. Since the xy plane always passes through the Earth, z_{earth} always equals zero.

The velocity of the object at impact takes into account only the component of Earth's velocity in the direction of the object's velocity at the time of impact. Therefore, the velocity in the xyz-frame at impact is:

$$v_x = (v_{x_{earth}} |\cos(\alpha + \phi)| - v \cos(\alpha + \phi)) \sin(\theta) \quad (3-16)$$

$$v_y = \left(v_{y_{earth}} |\sin(\alpha + \phi)| - v \sin(\alpha + \phi) \right) \sin(\theta) \quad (3-17)$$

$$v_z = -v \cos(\theta) \quad (3-18)$$

where $v_{x_{earth}}$ and $v_{y_{earth}}$ are components of the earth's velocity and v is the magnitude of the object's velocity at impact.

In order to determine the magnitude of the object's velocity at impact, an approximate model was created using Figure 3.2 of impact speeds for 411 existing long period comets.

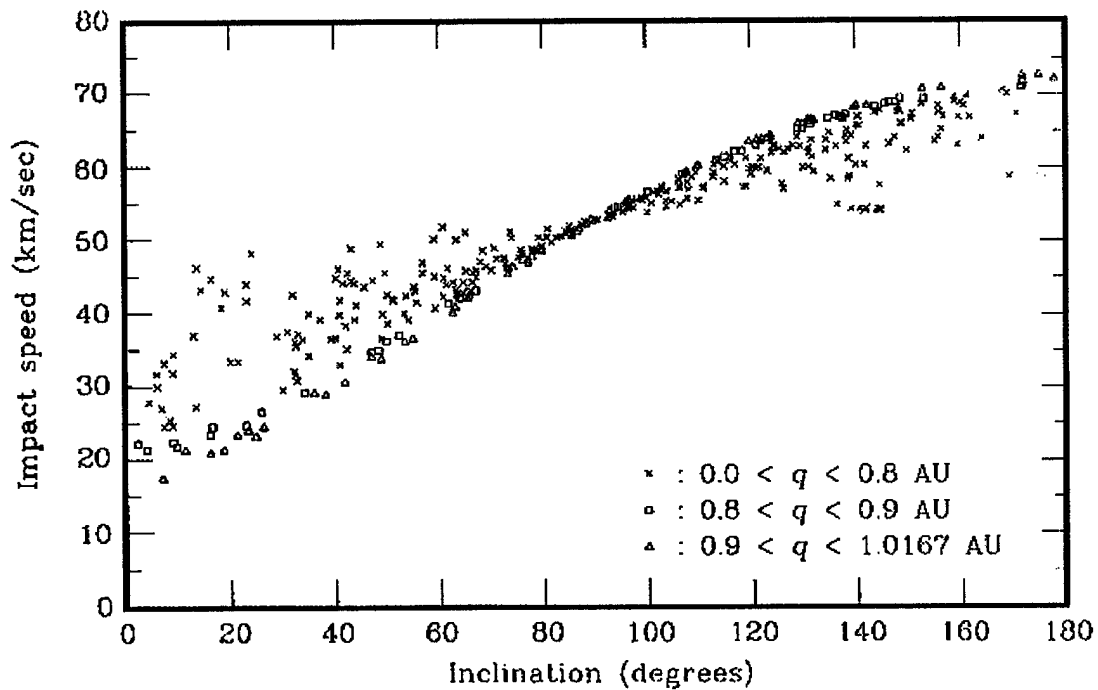


Figure 3.2. Terrestrial Impact Speeds for Observed Long Period Comets

For prograde trajectories, the speed at impact becomes:

$$v = 55 \text{ km/sec} - \left(1 - \frac{\text{inclination}}{90^\circ} \right) (r_{\text{perihelion}} * 38 \text{ km/sec}) \quad (3-19)$$

Likewise, for retrograde trajectories:

$$v = 55 \text{ km/sec} + \left(1 - \frac{\text{inclination}}{90^\circ}\right) (r_{\text{perihelion}} * 20 \text{ km/sec}) \quad (3-20)$$

where inclination is the inclination of the object's orbit, and $r_{\text{perihelion}}$ is the distance of the object from the sun at perihelion.

$r_{\text{perihelion}}$ for a prograde orbit is approximated with the following relation

$$r_{\text{perihelion}} = \cos(\phi - 270^\circ) \quad (3-21)$$

For a retrograde orbit, it is approximated by

$$r_{\text{perihelion}} = \cos(\phi - 90^\circ) \quad (3-22)$$

3.4 Integrating the Trajectory

Integration of the equations of variation and the equations of motion is accomplished using an ordinary differential equations integrator subroutine supplied by Dr. Wiesel. The subroutine Haming is a fourth order predictor-corrector algorithm. "...it carries the last four values of the state vector, and extrapolates these values to obtain a predicted next value, evaluates the equations of motion at the predicted point, and then corrects the extrapolated point using a higher order polynomial (18:120)." The subroutine Haming is utilized by subroutines Transfer, Bayes, and Check. To run, Haming requires an initial state vector and a time step. After a great deal of testing, a timestep of $dt = 0.001 \text{ days} = 86.400 \text{ seconds}$ was chosen. Using a time step of 8.64 seconds was slightly more accurate, however the error in the results is negligible.

3.5 Creating Observation Data

The Obser subroutine initially contained two types of observations. These included x,y,z data (for debugging purposes), and range and range rate data (17:Obser). For experimentation purposes, the following data types were added:

- Radar range data from the center of Earth
- Laser range data from the center of Earth
- Azimuth and elevation data from the center of Earth
- Azimuth and elevation data from 2 sites on opposite sides of the Earth's surface
- Azimuth and elevation data from a satellite in geosynchronous orbit
- Azimuth and elevation data from the center of the Moon
- Azimuth and elevation data from the center of Mars
- Azimuth, elevation, and radar range data from the center of Earth
- Azimuth and elevation data from the center of the Earth and geosynchronous orbit
- Azimuth and elevation data from the center of the Earth and the center of the Moon
- Azimuth and elevation data from the center of the Earth and the center of Mars
- Azimuth and elevation data from the center of the Earth and an orbit 90 degrees out of the Earth's orbital plane, 180 degrees out of phase, and a semi-major axis of 1 AU.

Azimuth and elevation measurements are assumed to have accuracies of ± 0.1 arcseconds. Radar range measurements have accuracies of ± 15 meters and laser range measurements have accuracies of ± 1 centimeter. The observational range of these instruments is not taken into account.

It is important to keep in mind that the number of observation discussed per day does not account for observational problems or interference. Such problems include weather, sun obscurement, mechanical failure, and scheduling conflicts. The reader should keep in mind that the observations involving two separate sources of data actually contains twice as much data for a given period of time. If the Mars and Earth combined data uses 10 observations per day, it is equivalent to 20 total observations per day. This will be discussed in more detail later.

3.6 The Bayes Filter

The Bayes Filter is an estimation algorithm similar to Least Squares but with an added benefit. For purposes of analysis, it was beneficial to sequentially add several days of data at a time and then run the estimation algorithm. Whereas all the old data must be reinput during each sequential iteration of Least Squares, with the Bayes Filter, it is only necessary to add new data. This is possible since the previous estimate should contain everything in the old data worth remembering, and a covariance matrix accompanies the previous estimate, which tells us how much the estimate can be trusted (19:94). The derivation that follows can be found in the MECH 731class text written by Dr. William E. Wiesel, pages 94 and 95.

The first step of the Bayes Filter algorithm is to bring in the old estimate (if one exists) and its covariance matrix to the new epoch. The observation relation for the new data, \bar{z} is:

$$\bar{z} = \vec{G}(\bar{x}, t) \quad (3-23)$$

The observation relation for the previous estimate, $\bar{x}(-)$, is:

$$\bar{x}(-) = I\bar{x} \quad (3-24)$$

The observation matrix for this set of data can be partitioned as

$$T = \begin{pmatrix} I \\ \dots \\ T_z \end{pmatrix} \quad (3-25)$$

with the subscript z referring to new data. The composite data covariance matrix is:

$$Q = \begin{pmatrix} P(-) & \phi \\ \phi & Q_z \end{pmatrix} \quad (3-26)$$

The zero blocks in the off diagonals demonstrate the independence of the old estimate and the new data. The residual vector is:

$$\bar{r} = \begin{pmatrix} \bar{x}(-) - \bar{x}_{ref} \\ \dots \\ \bar{z} - \bar{G}(\bar{x}) \end{pmatrix} \quad (3-27)$$

The previous step is used exclusively by the Bayes Filter. To find the new estimate, $\bar{x}(+)$, the same method as Least Squares is now used. The first matrix product is given by:

$$T^T Q^{-1} = (I, T_z^T) \begin{pmatrix} P^{-1}(-) & \phi \\ \phi & Q_z^{-1} \end{pmatrix} = (P^{-1}(-), T_z^T Q_z^{-1}) \quad (3-28)$$

The inverse of the new estimate's covariance is given by:

$$P^{-1}(+) = (P^{-1}(-), T_z^T Q_z^{-1}) \begin{pmatrix} I \\ \dots \\ T_z \end{pmatrix} = P^{-1}(-) + T_z^T Q_z^{-1} T_z \quad (3-29)$$

The correction becomes:

$$\delta\bar{x}(t_o) = P(+)^T Q^{-1} \bar{r} = P(+)(P^{-1}(-)(\bar{x}(-) - \bar{x}_{ref}) + T_z^T Q_z^{-1} \bar{r}_z) \quad (3-30)$$

and the new estimate:

$$\bar{x}(+) = \bar{x}(-) + \delta\bar{x}(t_o) \quad (3-31)$$

Once the epoch is brought to a new time, the old estimate is considered to be data, and no further changes are allowed. The role of the old covariance matrix $P^{-1}(-)$ is as a weighting matrix for the state residuals. If the old estimate is good, the covariance matrix will be large and the state residuals will not be allowed to grow relatively large. If the old estimate is bad, the covariance matrix will be small and the new estimate will be less constrained to resemble the old estimate (18: 96).

3.7 Impact Prediction

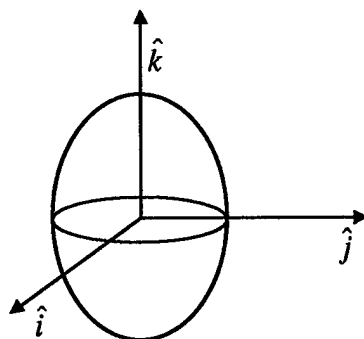


Figure 3.3. Error Ellipsoid in the XYZ-Frame

In order to properly predict whether or not the object impacts with the Earth, close attention must be paid to the error ellipsoids. More specifically, we are concerned with the positional error ellipsoid. The subroutine Check accomplishes the process described in this section.

In order to determine the error ellipsoid, the state covariance matrix at the time t_o , $P_x(t_o)$, must be propagated to the final time when it becomes $P_x(t_f)$. This is accomplished using the relation:

$$P_x(t_f) = \Phi(t, t_o) P_x(t_o) \Phi^T(t_f, t_o) \quad (3-32)$$

where Φ is the state transition matrix (19:34). The state transition matrix propagates the actual state as a function of time, not the differential of the state (19:33).

Both P and Φ are 6x6 matrices. The portion of the final state covariance matrix we want is the upper left 3x3, which contains the "spatial" information. To remove the positional error ellipsoid from this 3x3 matrix, the eigenvalues must be calculated. Calculating the eigenvalues of this matrix will furnish us with the one-sigma impact ellipsoid (19:46).

To transfer the error ellipsoid into a more useful form, it must be transformed into a more convenient frame. The frame chosen is one based on the normal of the object's velocity vector, \vec{v} , which will be the unit vector, \hat{e}_1 .

$$\hat{e}_1 = \frac{\vec{v}}{\|\vec{v}\|} \quad (3-33)$$

The next axis will be defined as a unit vector perpendicular to \hat{e}_1 in the direction of \hat{k} shown in Figure 3.1 and Figure 3.3. So the amount of \hat{e}_1 that is in the \hat{k} direction is subtracted from \hat{k} .

$$\hat{e}_2 = \frac{\hat{k} - (\hat{k} \cdot \hat{e}_1) \hat{e}_1}{\|\hat{k} - (\hat{k} \cdot \hat{e}_1) \hat{e}_1\|} \quad (3-34)$$

For the final axis the easiest route is to take the cross product of the first two in order to insure orthogonality.

$$\hat{e}_3 = \hat{e}_1 \times \hat{e}_2 \quad (3-35)$$

This direction ends up pointing eastward on the Earth at the time of impact.

We can now define the xyz to e-frame rotation matrix:

$$R = [\hat{e}_1 \quad \hat{e}_2 \quad \hat{e}_3] \quad (3-36)$$

Each of the unit vectors has three components in the xyz-frame, resulting in a 3x3 rotation matrix that can transfer the error ellipsoid to the e-frame. Not only is this form easier to use, but also demonstrates the large amount of uncertainty that exists in the direction of the velocity compared to the small amount in the other directions.

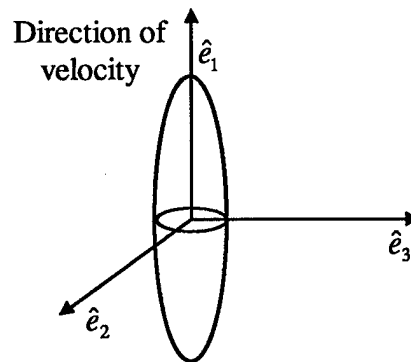


Figure 3.4. Error Ellipsoid in the E-Frame

Data will be added to the Bayes Filter in increments of 10 or 5 days depending on the magnitude of the previous error ellipsoid. The end result of each Bayes Filter run is then propagated forward in time to determine whether a positive impact can be determined. At closest approach to the Earth (or impact), the error ellipsoid is analyzed and then

plotted on a circle representing the relative size and position of the Earth. To analyze the error ellipsoid, the extreme points of the ellipsoid are propagated forward in time to determine if the object would still impact the Earth if it were located at the extremes of the positional error ellipsoid. The time at which the error ellipsoid becomes small enough to positively determine an impact is calculated with a great deal of error (less than 10 days and most likely less than 5 days), but this is sufficient for the sensitivity analysis the results are intended for.

IV. Results and Analysis

This section is dedicated to the execution of the program created for this thesis, given various final impact parameters. The output of the program will be displayed, discussed, and analyzed in order to develop a better understanding of extreme examples of what can happen as well as sensitivity of examples to various parameters. Unless otherwise specified, optical (azimuth and elevation) data is used, and will be taken in 10-day increments with 10 observations per day. In addition, an accuracy of 0.1 arcseconds is used. Typical optical tracking accuracy using state of the art equipment lies in between 1.0 arcseconds and 0.1 arcseconds.

4.1 The Extreme Trajectories

To set the stage for further analysis, it is beneficial to first take a look at the limits of what can happen. For this reason, the first section will be dedicated to examining the extreme trajectories. Not only will this demonstrate the least amount of time before impact for determining whether an object will impact with Earth, but also the longest amount.

4.1.1 Trajectory 1. The impact conditions of this case include an impact velocity of 53.0 km/sec, $\phi=0.0^\circ$, $\theta=90.0^\circ$.

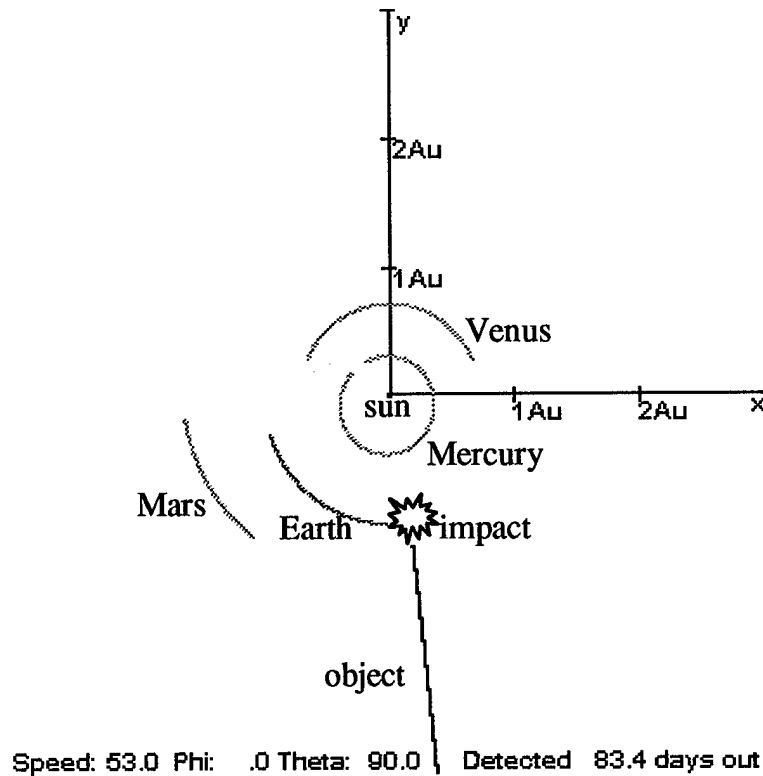


Figure 4.1. Trajectory 1 (Overhead View)

This results in an orbit that would pass through the sun if Earth were not in the way, as illustrated in Figure 4.1. It isn't a very feasible case, however, it does represent a good worst case scenario. Added to this, objects have been known to pass extremely close to the sun, so slight offsets to this orbit are feasible.

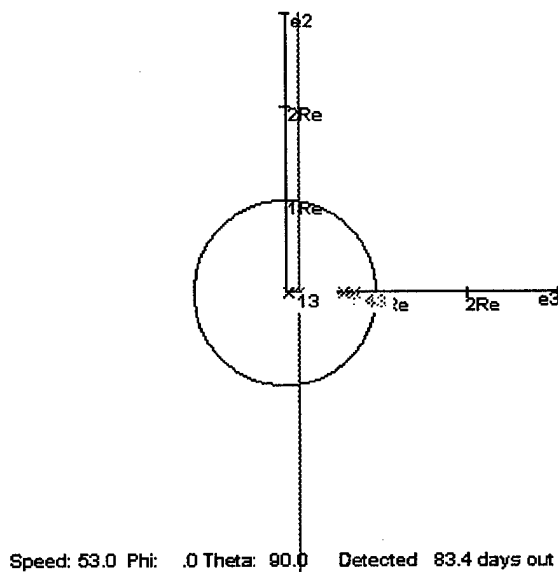


Figure 4.2. Error Ellipsoid (Velocity In, North Up)

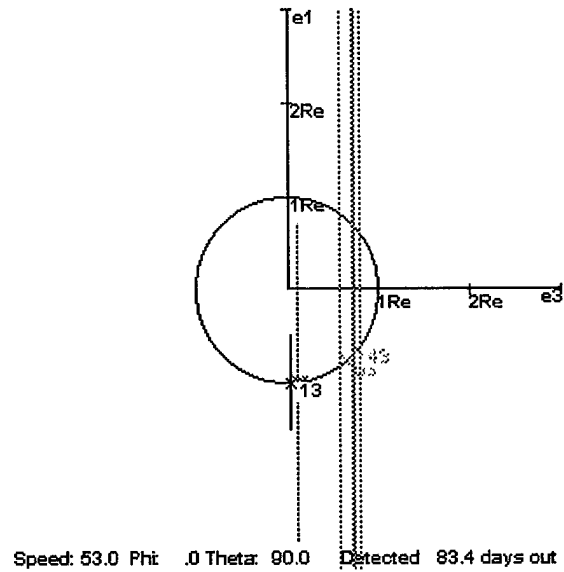


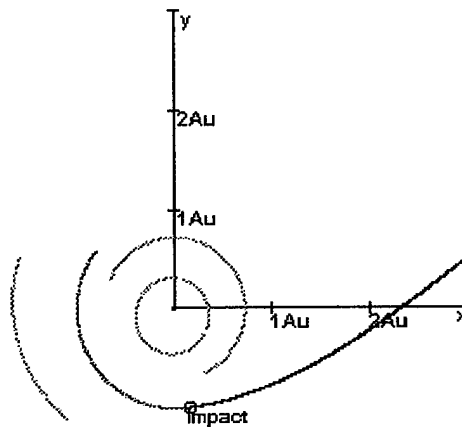
Figure 4.3. Error Ellipsoid (Velocity Up, North Out)

The error ellipsoid plots in Figures 4.2 and 4.3 show the results of sequential 10-day iterations. This is done to examine how the error ellipsoids change as more data is added and the estimate becomes more accurate. It is fairly apparent that the largest amount of uncertainty is and will always be in the direction of the velocity. This is because of the type of data used. Using optical data, azimuth and elevation can be found with fairly good accuracy (.1 arcseconds), however, nothing is known about the range. The uncertainty in the range almost always translates to uncertainty in position in the velocity direction at impact. The exceptions involve a large change in the direction of the velocity between the time the observations are taken, and the time of impact.

For this trajectory, if no steps were taken prior to confirming a future impact, there would only be 13 days to react. This is a very short amount of time for a deflection to be attempted. It should be noted, however, that with only 10 days of data, it can be

determined that this object will pass within 154 Earth radii of Earth. This is an excellent indicator that it is a good time to begin taking more data.

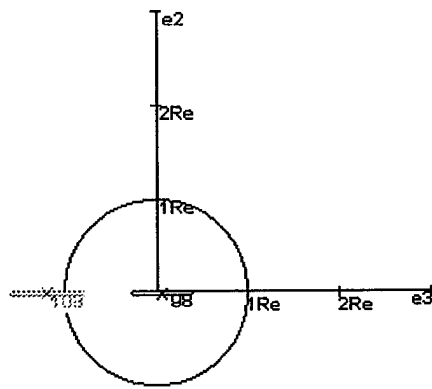
4.1.2 Trajectory 2. The impact conditions of trajectory 2 include an impact velocity of 78.0 km/sec, $\phi=90.0^\circ$, $\theta=90.0^\circ$.



Speed: 78.0 Phi: 90.0 Theta: 90.0 Detected 138.3 days out

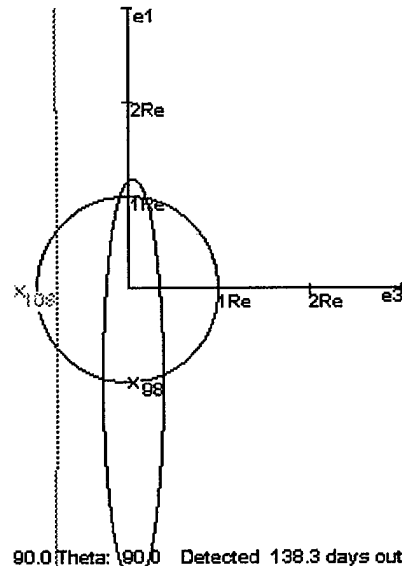
Figure 4.4. Trajectory 2 (Overhead View)

Like trajectory 1, this orbit has almost no inclination, however, this trajectory is retrograde with respect to the Earth's orbit. As can be seen in the trajectory plot in Figure 4.4, the NEO impacts with Earth head-on. This means that their velocities are in exactly opposite directions at the time of impact. The most important thing to remember about this trajectory is that retrograde trajectories will almost always have a higher velocity and thus more kinetic energy at impact.



Speed: 78.0 Phi: 90.0 Theta: 90.0 Detected 138.3 days out

Figure 4.5. Error Ellipsoid (Velocity In, North Up)



Speed: 78.0 Phi: 90.0 Theta: 90.0 Detected 138.3 days out

Figure 4.6. Error Ellipsoid (Velocity Up, North Out)

The benefit of this orbit, as seen in the error ellipsoid plots, is that a future impact can be determined while the error ellipsoid is still very large. This is due to the fact that the Earth and the NEO are traveling in relatively straight paths over a large distance before impact. For this reason, as long as the two bodies are in-line with each other and the majority of the uncertainty in position is in the direction of the object's velocity, an impact prediction is fairly easy. This prediction only took 40 days, leaving 98 days to react.

4.1.3 Trajectory 3. The impact conditions of trajectory 3 include an impact velocity of 53.0 km/sec, $\phi=180.0^\circ$, $\theta=90.0^\circ$.

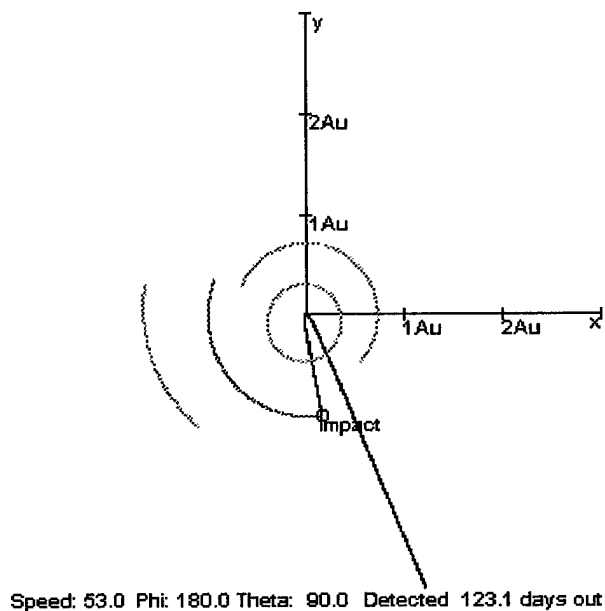


Figure 4.7. Trajectory 3 (Overhead View)

Once again, this orbit has almost no inclination. The most noteworthy thing about this orbit is that it passes extremely close to the sun. The result of the object's close encounter with the Sun is that it performs a near 180 turn and heads back nearly the same way it came.

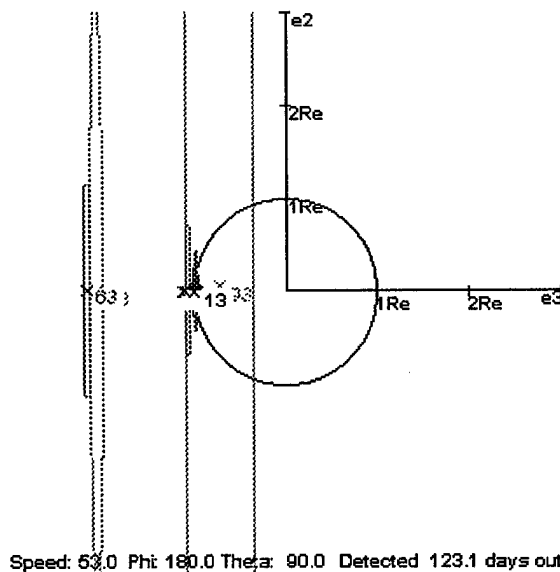


Figure 4.8. Error Ellipsoid (Velocity In, North Up)

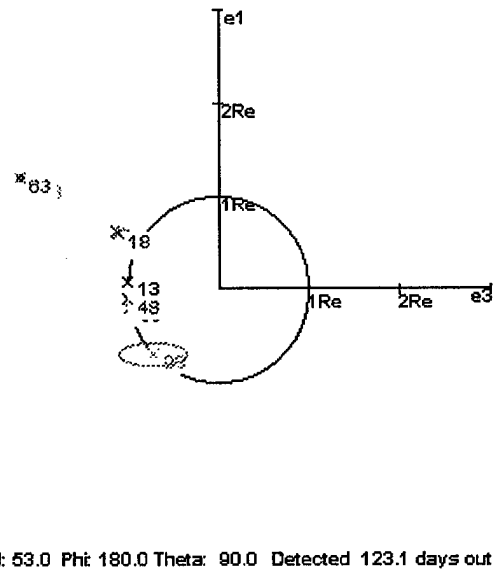
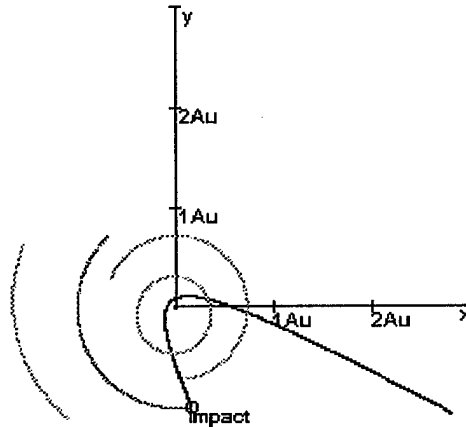


Figure 4.9. Error Ellipsoid (Velocity Up, North Out)

The error ellipsoids for this trajectory seem to be very erratic, most likely because they are. The closer an object passes to a large body, the harder it is to accurately model its future path through space. This can be looked at from a chaotic dynamics aspect in that tiny variations in initial conditions can cause very large differences in the final outcome. The closer the object flies past a large body, the more this is true.

The worst aspect of this trajectory concerning detection and defense is that it comes at the Earth right out of the Sun. Therefore, optical observations must be taken before the object's proximity to the Sun makes it impossible to see. It would be very difficult to make optical observations on the final leg of the object's orbit before impact, since from the Earth's point of view, the object would remain nearly aligned with the Sun.

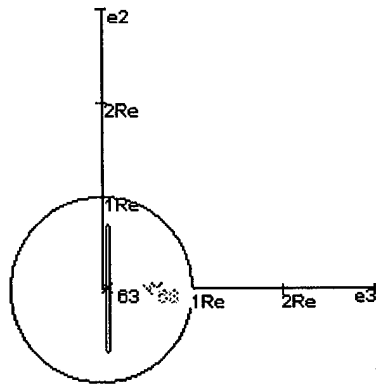
4.1.4 Trajectory 4. The impact conditions of trajectory 4 include an impact velocity of 46.4 km/sec, $\phi=190.0^\circ$, $\theta=90.0^\circ$.



Speed: 46.4 Phi: 190.0 Theta: 90.0 Detected 148.6 days out

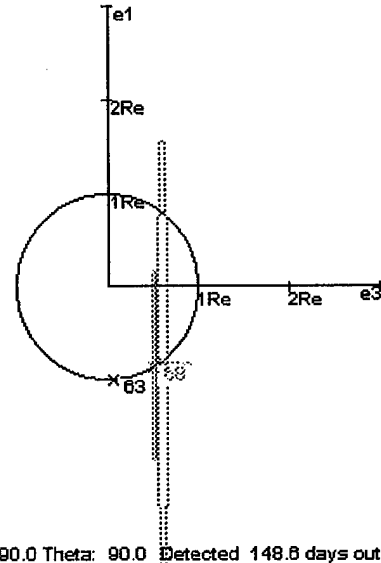
Figure 4.10. Trajectory 4 (Overhead View)

After examining trajectory 3, it was apparent that testing a similar trajectory might shed light on the sensitivity of impact predictions to large body interactions. This trajectory remains near Earth's orbital plane, however, it does not pass as close to the Sun as trajectory 4.



Speed: 46.4 Phi: 190.0 Theta: 90.0 Detected 148.6 days out

Figure 4.11. Error Ellipsoid (Velocity In, North Up)

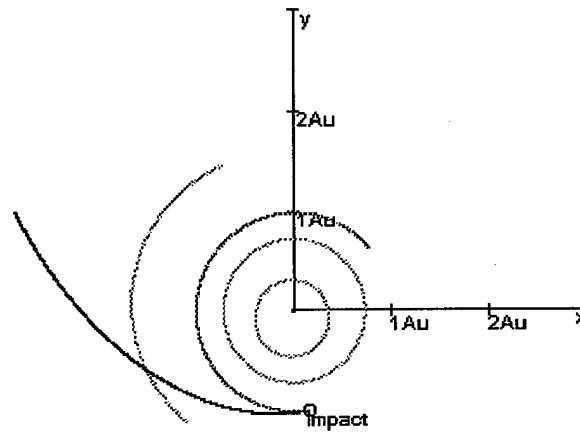


Speed: 46.4 Phi: 190.0 Theta: 90.0 Detected 148.6 days out

Figure 4.12. Error Ellipsoid (Velocity Up, North Out)

The error ellipsoids in Figures 4.11 and 4.12 demonstrate that this trajectory is much more favorable to accurately predicting an impact.

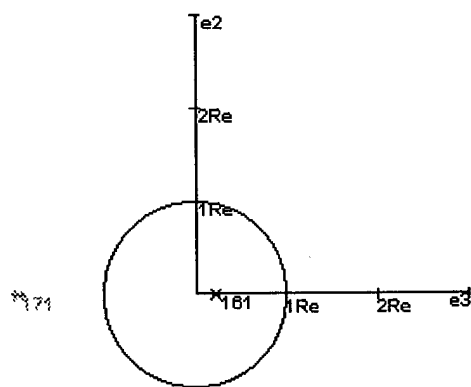
4.1.5 Trajectory 5. The impact conditions of trajectory 5 include an impact velocity of 15.0 km/sec, $\phi=270.0^\circ$, $\theta=90.0^\circ$.



Speed: 15.0 Phi: 270.0 Theta: 90.0 Detected 241.0 days out

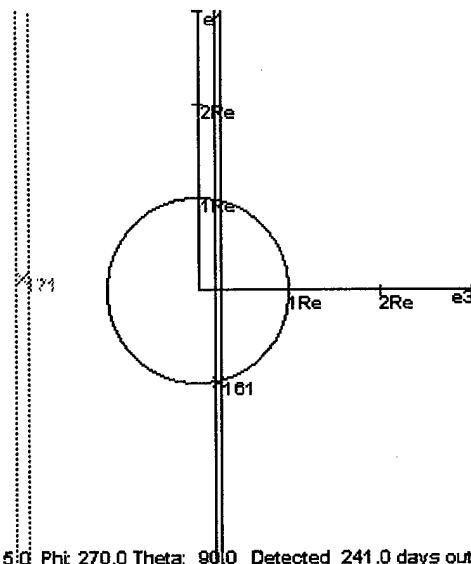
Figure 4.13. Trajectory 5 (Overhead View)

The important aspect of this trajectory is that the Earth and the NEO are traveling in the exact same direction at impact. This trajectory has the benefit of vastly reducing the amount of kinetic energy the NEO has at impact. As you can see, the impact velocity is only 15.0 km/sec as opposed to 78.0 km/sec when the Earth and NEO impact head-on.



Speed: 15.0 Phi: 270.0 Theta: 90.0 Detected 241.0 days out

Figure 4.14. Error Ellipsoid (Velocity In, North Up)

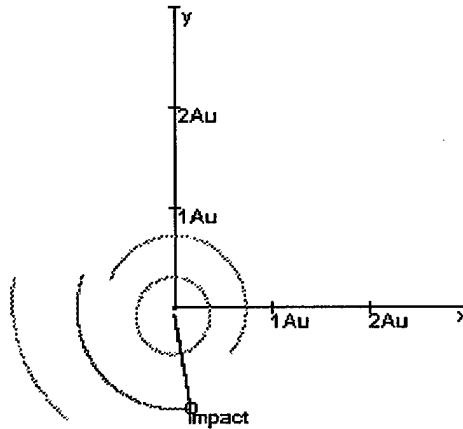


Speed: 15.0 Phi: 270.0 Theta: 90.0 Detected 241.0 days out

Figure 4.15. Error Ellipsoid (Velocity Up, North Out)

Like trajectory 2, a future impact can be determined while the error ellipsoid is still very large. This trajectory is similar to trajectory 2 in that the Earth and NEO are both traveling in a relatively straight path over a considerable path before impact, making impact prediction a painless task. This impact is determined in 40 days, leaving 161 days for reaction.

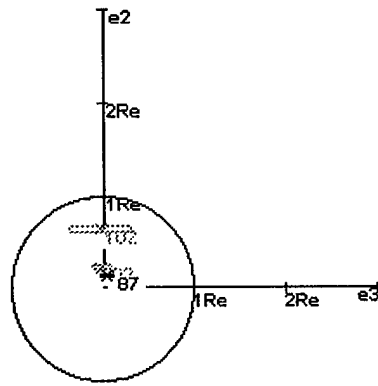
4.1.6 Trajectory 6. The impact conditions of trajectory 6 include an impact velocity of 53.0 km/sec, $\phi=0.0^\circ$, $\theta=180.0^\circ$.



Speed: 53.0 Phi: .0 Theta: 180.0 Detected 122.2 days out

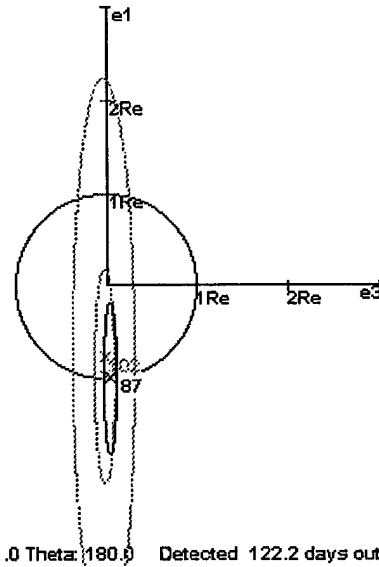
Figure 4.16. Trajectory 6 (Overhead View)

This trajectory ultimately results in a impact at the north pole (approximately), headed straight south. This orbit is inclined 90° .



Speed: 53.0 Phi: .0 Theta: 180.0 Detected 122.2 days out

Figure 4.17. Error Ellipsoid (Velocity In, North Up)

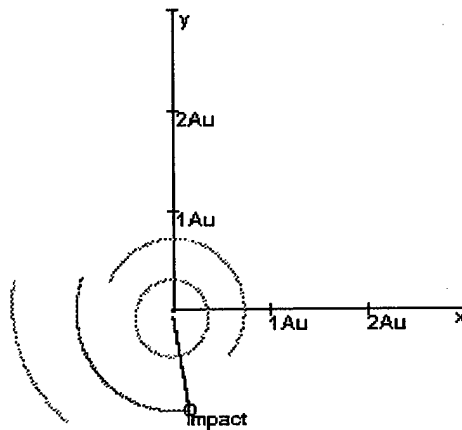


Speed: 53.0 Phi: .0 Theta: 180.0 Detected 122.2 days out

Figure 4.18. Error Ellipsoid (Velocity Up, North Out)

As illustrated in Figures 4.17 and 4.18, for this trajectory, it is fairly easy to quickly and accurately predict an impact. This is primarily true because when taking measurements of a body that lies far out of the Earth's plane if the body is relatively close, the movement of the Earth will provide a great means of triangulation. This vastly cuts down on the uncertainty in range discussed earlier. For trajectory 6, the NEO is detected 122 days before impact, and the future impact is positively identified 87 days before impact.

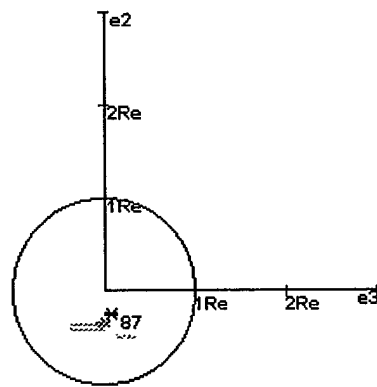
4.1.7 Trajectory 7. The impact conditions of trajectory 7 include an impact velocity of 53.0 km/sec, $\phi=0.0^\circ$, $\theta=0.0^\circ$.



Speed: 53.0 Phi: .0 Theta: .0 Detected 122.2 days out

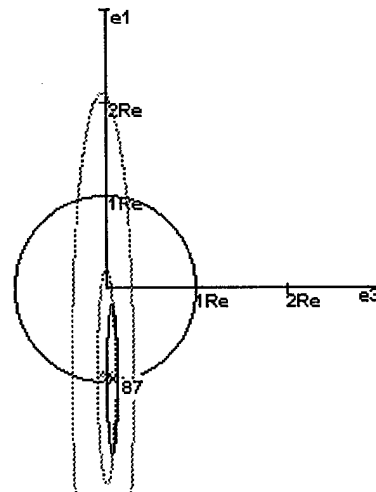
Figure 4.19. Trajectory 7 (Overhead View)

The trajectory shown in Figure 4.19 is the opposite of the last trajectory, in that it impacts the south pole of the Earth headed due north.



Speed: 53.0 Phi: .0 Theta: .0 Detected 122.2 days out

Figure 4.20. Error Ellipsoid (Velocity In, North Up)



Speed: 53.0 Phi: .0 Theta: .0 Detected 122.2 days out

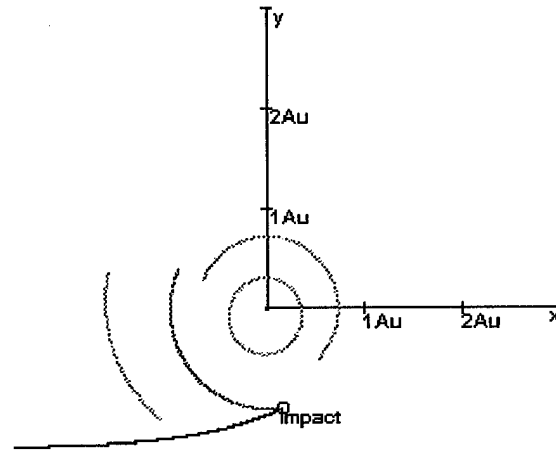
Figure 4.21. Error Ellipsoid (Velocity Up, North Out)

As expected, the plots of the error ellipsoids for trajectory 7 look very similar to those of trajectory 6. Again, the object is detected at 122 days and the future impact is positively identified 87 days before impact.

4.2 Sensitivity Analysis

One of the initial objectives of this thesis was not to settle for mere impact predictions, but to take the next step and monitor the sensitivity of impact prediction to changes in parameters within our control. These parameters include: amount of data, accuracy of data, type of data, location of data source, combinations of types of data, and combinations of data sources.

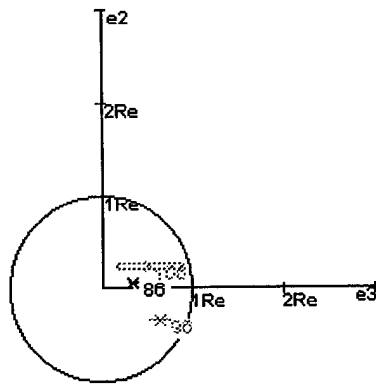
4.2.1 Trajectory 8. The impact conditions of trajectory 8 include an impact velocity of 29.2 km/sec, $\phi=300.0^\circ$, $\theta=65.0^\circ$.



Speed: 29.2 Phi: 300.0 Theta: 65.0 Detected 126.1 days out

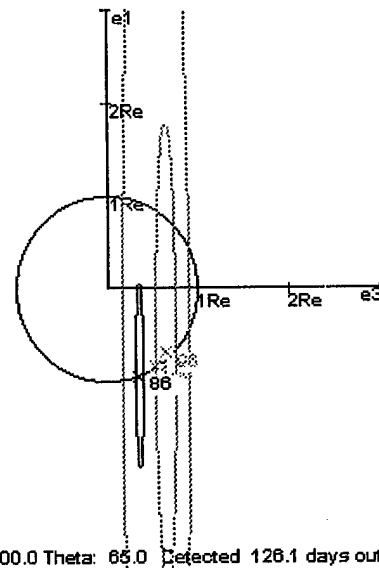
Figure 4.22. Trajectory 8 (Overhead View)

This is a prograde trajectory that impacts the Earth before perigee. The trajectory 8 orbit is inclined 25.0° relative to the Earth's orbit. This trajectory was selected at random, in an effort to avoid extremes and present a realistic example. For example, although Oort Cloud comets' inclinations are randomly scattered, the affects of a high inclination on analysis have already been demonstrated, so a trajectory which would be harder to determine an impact for was selected.



Speed: 29.2 Phi: 300.0 Theta: 65.0 Detected 126.1 days out

Figure 4.23. Error Ellipsoid (Velocity In, North Up)

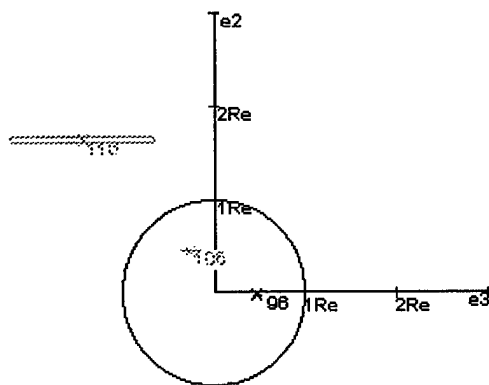


Speed: 29.2 Phi: 300.0 Theta: 65.0 Detected 126.1 days out

Figure 4.24. Error Ellipsoid (Velocity Up, North Out)

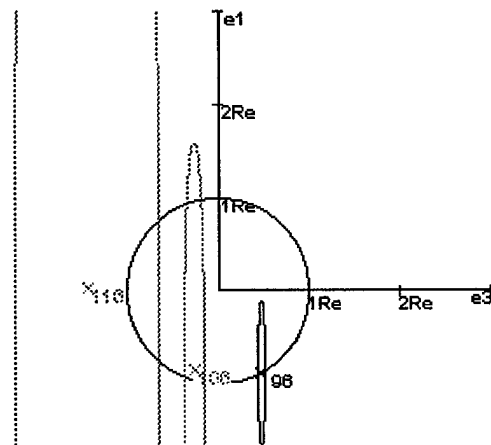
As demonstrated in the error ellipsoid in Figures 4.23 and 4.24, impact determination for this orbit is neither too easy nor too difficult. The object is detected at 3.0 AU, 126 days before impact, and a positive future impact is determined in approximately 40 days, leaving 86 days to react.

4.2.1.1 100 Observations Per Day.



Speed: 29.2 Phi: 300.0 Theta: 65.0 Detected 126.1 days out

Figure 4.25. Error Ellipsoid (Velocity In, North Up)

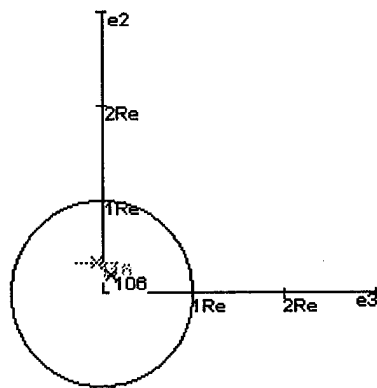


Speed: 29.2 Phi: 300.0 Theta: 65.0 Detected 126.1 days out

Figure 4.26. Error Ellipsoid (Velocity Up, North Out)

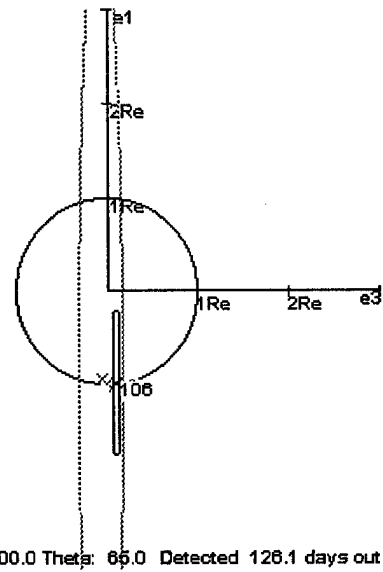
Increasing the number of data points per day from 10 to 100 significantly improves the ability to accurately predict future impacts. In this case, the time it takes to positively identify a future impact decreases by 10 days. It may not seem like much, however, when deciding how to react to a possible catastrophe, every second counts.

4.2.1.2 1000 Observations Per Day.



Speed: 29.2 Phi: 300.0 Theta: 65.0 Detected 126.1 days out

Figure 4.27. Error Ellipsoid (Velocity In, North Up)

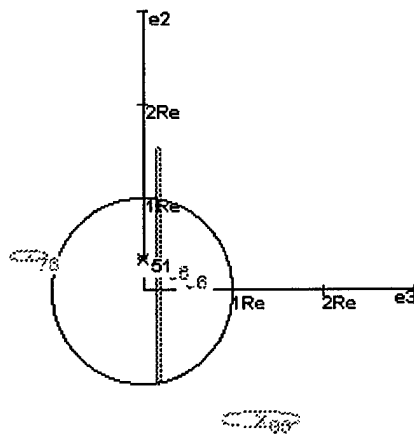


Speed: 29.2 Phi: 300.0 Theta: 65.0 Detected 126.1 days out

Figure 4.28. Error Ellipsoid (Velocity Up, North Out)

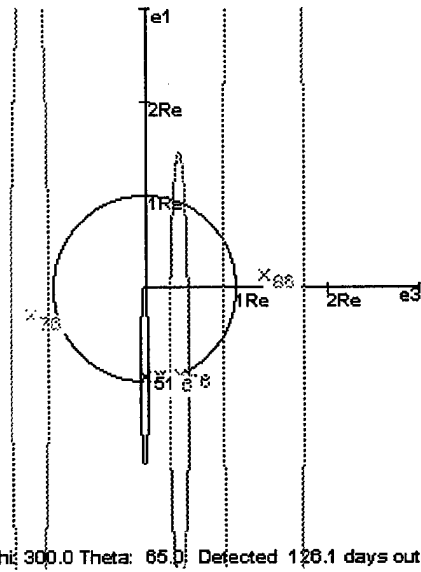
Whereas increasing the number of observations from 10 per day to 100 per day improved the impact warning time by 10 days, increasing the observations from 10 per day to 1000 per day only increases the impact warning time by 20 days. This demonstrates a tradeoff which must be made between the cost required to accomplish a particular number of observations, and the associated warning times.

4.2.1.3 1.0 Arcsecond Accuracy.



Speed: 29.2 Phi: 300.0 Theta: 65.0 Detected 126.1 days out

Figure 4.29. Error Ellipsoid (Velocity In, North Up)

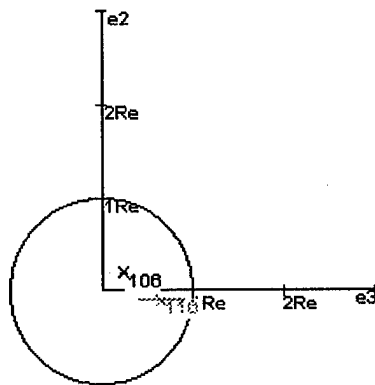


Speed: 29.2 Phi: 300.0 Theta: 65.0 Detected 126.1 days out

Figure 4.30. Error Ellipsoid (Velocity Up, North Out)

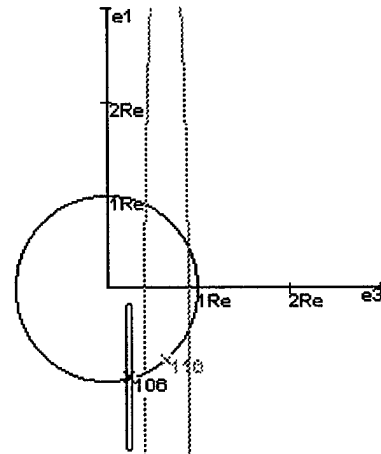
Figures 4.29 and 4.30 demonstrate that a reduction in accuracy of the azimuth and elevation angular data from 0.1 arcseconds to 1.0 arcseconds has a very detrimental effect on the impact warning time. When comparing the error ellipsoids of the 1.0 arcsecond accuracy data to the 0.1 arcsecond accuracy data, its easy to see why the reduction in observation accuracy is not acceptable, especially with the associated consequences of a large delay in impact prediction. In this case, the warning time decreases from 86 days to 51 days, over a month less time to react.

4.2.1.4 0.01 Arcsecond Accuracy.



Speed: 29.2 Phi: 300.0 Theta: 65.0 Detected 126.1 days out

Figure 4.31. Error Ellipsoid (Velocity In, North Up)



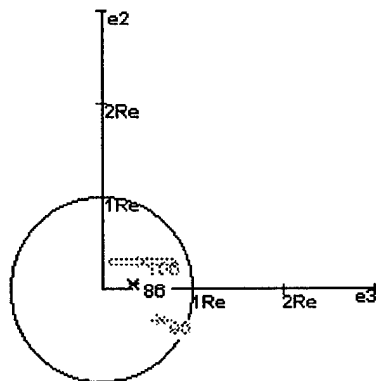
Speed: 29.2 Phi: 300.0 Theta: 65.0 Detected 126.1 days out

Figure 4.32. Error Ellipsoid (Velocity Up, North Out)

By increasing the accuracy from 0.1 arcseconds to 0.01 arcseconds, the impact warning time increases as would be expected. An interesting note, however, is that by increasing the accuracy by a factor of 10 the warning time increases by 20 days, but by decreasing the warning time by a factor of 10, the warning time decreases by 35 days.

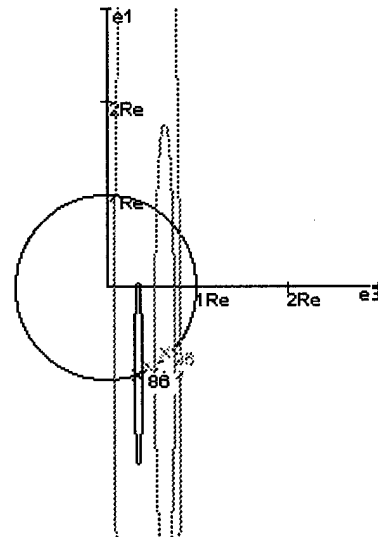
4.2.1.5 Observations from 2 Sites Rotating on the Surface of the Earth. This type of observational data was created to demonstrate whether or not the rotation of the Earth aids in the triangulation of NEOs. As can be expected, the results look exactly like the results of using data originating from the center of the Earth. The movement of the Earth in the solar system negates the affects of any movement on the part of the rotation of an observation site on the surface of the Earth.

4.2.1.6 Observations from Geosynchronous Orbit.



Speed: 29.2 Phi: 300.0 Theta: 65.0 Detected 126.1 days out

Figure 4.33. Error Ellipsoid (Velocity In, North Up)

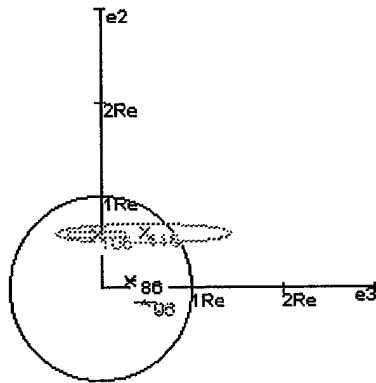


Speed: 29.2 Phi: 300.0 Theta: 65.0 Detected 126.1 days out

Figure 4.34. Error Ellipsoid (Velocity Up, North Out)

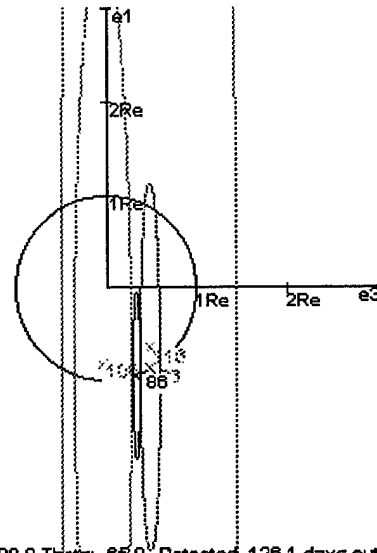
Using geosynchronous orbit data does not improve the impact prediction. This type of data was created to identify whether or not satellites in a geosynchronous orbit could be helpful in determining impacts. This and the next two data types were created to determine at what distance from the Earth that the data source's orbit would provide beneficial triangulation of the NEO being observed.

4.2.1.7 Observations from the Moon.



Speed: 29.2 Phi: 300.0 Theta: 65.0 Detected 126.1 days out

Figure 4.35. Error Ellipsoid (Velocity In, North Up)

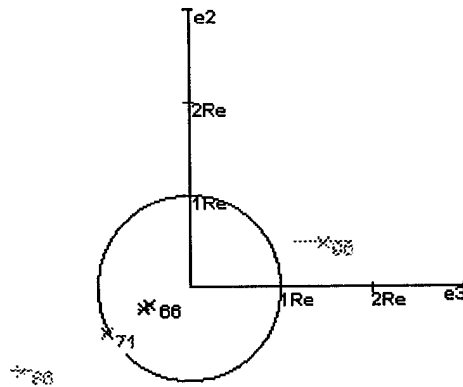


Speed: 29.2 Phi: 300.0 Theta: 65.0 Detected 126.1 days out

Figure 4.36. Error Ellipsoid (Velocity Up, North Out)

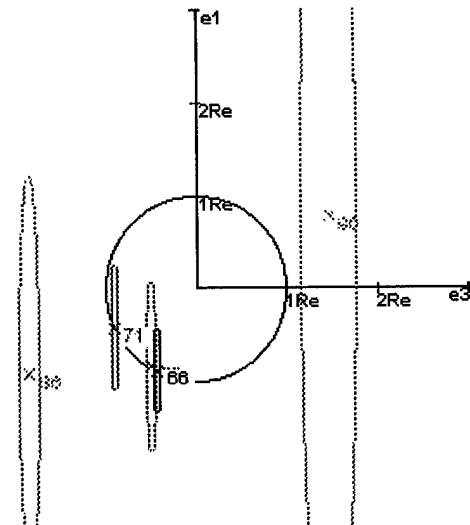
The error ellipsoid plots in Figures 4.35 and 4.36 illustrate that although the early iterations converge more quickly on the Earth, the error ellipsoid at 86 days is almost exactly the same. The moon apparently does help with impact prediction, but the improvement is insignificant. The cost would probably not be worth placing an observing device on the moon.

4.2.1.8 Observations from Mars.



Speed: 29.2 Phi: 300.0 Theta: 65.0 Detected 126.1 days out

Figure 4.37. Error Ellipsoid (Velocity In, North Up)

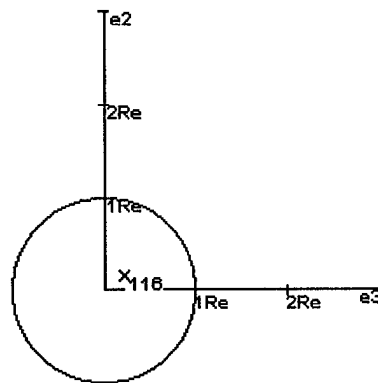


Speed: 29.2 Phi: 300.0 Theta: 65.0 Detected 126.1 days out

Figure 4.38. Error Ellipsoid (Velocity Up, North Out)

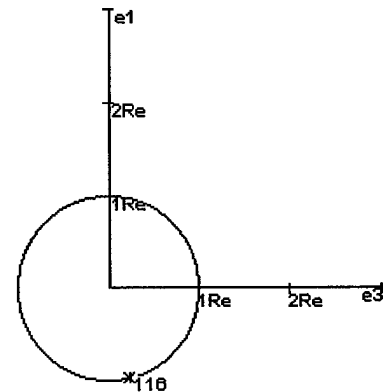
The results of the run using data originated from Mars alone actually reduces our ability to accurately predict an impact. The effectiveness of this type of data depends almost entirely on the position of Mars with respect to the object. There are many situations in which data from the Earth will be much better, however, if the object passes anywhere near Mars on its way to Earth, the Mars data will most likely be better.

4.2.1.9 Range, Azimuth, and Elevation Observations from Earth.



Speed: 29.2 Phi: 300.0 Theta: 65.0 Detected 126.1 days out

Figure 4.39. Error Ellipsoid (Velocity In, North Up)

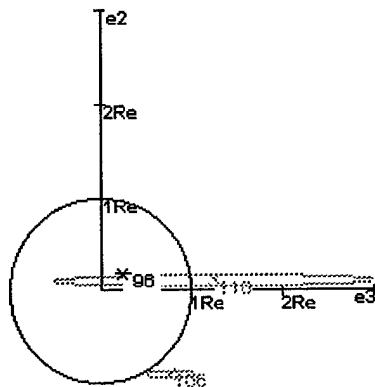


Speed: 29.2 Phi: 300.0 Theta: 65.0 Detected 126.1 days out

Figure 4.40. Error Ellipsoid (Velocity Up, North Out)

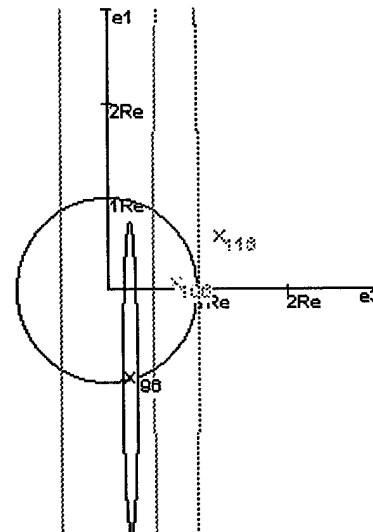
As discussed previously, when the program is executed, an initial number of days of data to be used by the Bayes Filter for the first iteration is inputted to the program. This value is altered depending on the type of trajectory. The lowest this value has been set so far is 10. In this case, 10 days is more than enough to not only predict and impact, but to do so with an insignificant error ellipsoid. The vastly improved accuracy is due to the fact that the uncertainty in the range of the NEO that has consistently eluded our azimuth and elevation data suddenly has disappeared. The tremendous amount of power needed to make these range observations, and the actual range of such an observational device is another matter as demonstrated in Table 2.2.

4.2.1.10 Observations from Earth and Geosynchronous Orbit.



Speed: 29.2 Phi: 300.0 Theta: 65.0 Detected 126.1 days out

Figure 4.41. Error Ellipsoid (Velocity In, North Up)

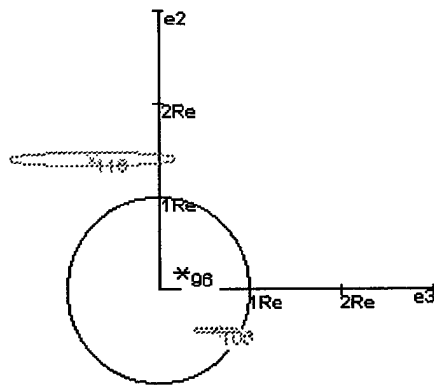


Speed: 29.2 Phi: 300.0 Theta: 65.0 Detected 126.1 days out

Figure 4.42. Error Ellipsoid (Velocity Up, North Out)

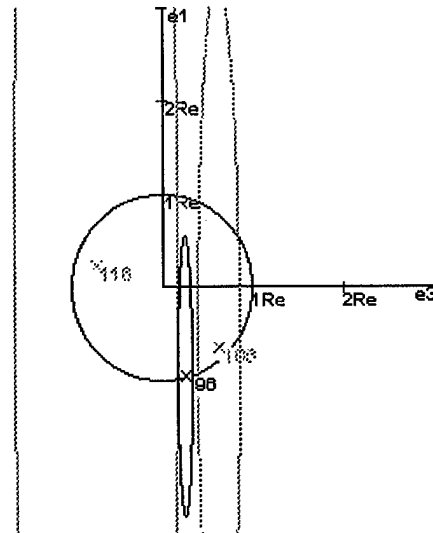
This type of data combination provides an entirely new outlook on data sources. Instead of having to wait for movement within the orbit of the body providing observations, constant triangulation is provided by using Earth centered data at the same time. The only flaw with this combination is that 20 data points are produced per day instead of 10. Knowing this, and knowing how little data originating in a geosynchronous orbit improves impact prediction, the improvement in this type of data is mostly due to the increased number of data points used.

4.2.1.11 Observations from Earth and the Moon.



Speed: 29.2 Phi: 300.0 Theta: 65.0 Detected 126.1 days out

Figure 4.43. Error Ellipsoid (Velocity In, North Up)

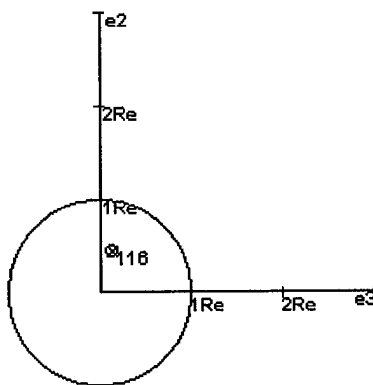


Speed: 29.2 Phi: 300.0 Theta: 65.0 Detected 126.1 days out

Figure 4.44. Error Ellipsoid (Velocity Up, North Out)

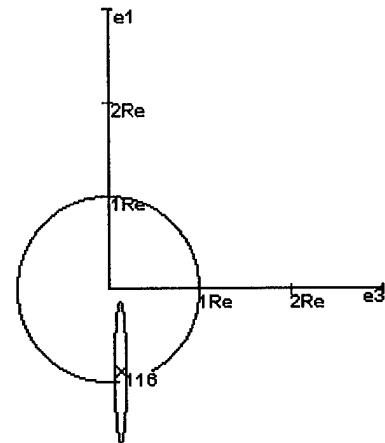
As with the Moon only observations, the initial data is improved, however, the actual positive impact prediction remains approximately the same. The only improvement is due to the increase in the number of observations per day as with the combined Earth and geosynchronous orbit data.

4.2.1.12 Observations from Earth and Mars.



Speed: 29.2 Phi: 300.0 Theta: 65.0 Detected 126.1 days out

Figure 4.45. Error Ellipsoid (Velocity In, North Up)

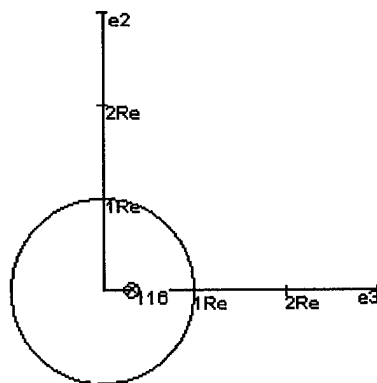


Speed: 29.2 Phi: 300.0 Theta: 65.0 Detected 126.1 days out

Figure 4.46. Error Ellipsoid (Velocity Up, North Out)

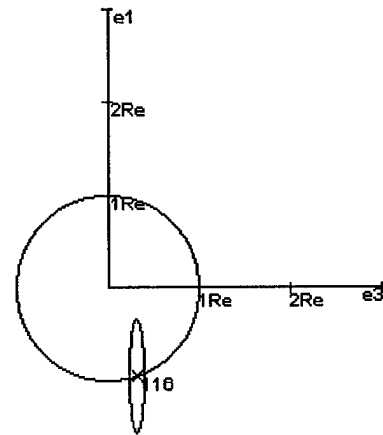
Unlike the run where Mars data was the only source, once Earth data and Mars data are combined, the time necessary to predict an impact drops considerably. Even though the data from either source may not be excellent quality, the data from the two separate sources can be triangulated with a large degree of accuracy due to the distance separation between the two bodies.

4.2.1.13 Observations from Earth and an Out of Plane Orbit.



Speed: 29.2 Phi: 300.0 Theta: 65.0 Detected 126.1 days out

Figure 4.47. Error Ellipsoid (Velocity In, North Up)

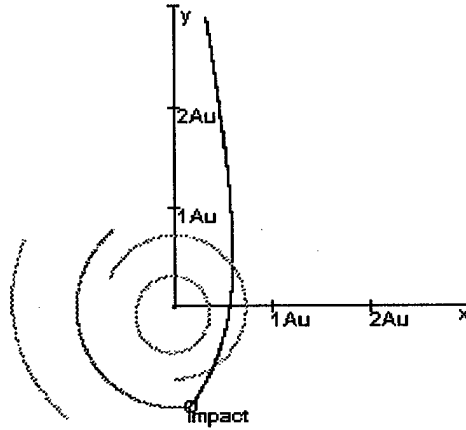


Speed: 29.2 Phi: 300.0 Theta: 65.0 Detected 126.1 days out

Figure 4.48. Error Ellipsoid (Velocity Up, North Out)

This type of data combination vastly improves impact prediction. It is similar to using combined Mars and Earth data, however, the way the orbit is set up, it ensures a large line of sight separation between the satellite and Earth at any given time. The closest the satellite ever is to the Earth is 1.414 AU, and since the satellite is in an orbit with an inclination of 90° , chances are good that observations will have fairly large angular differences between the sources within 3 AU.

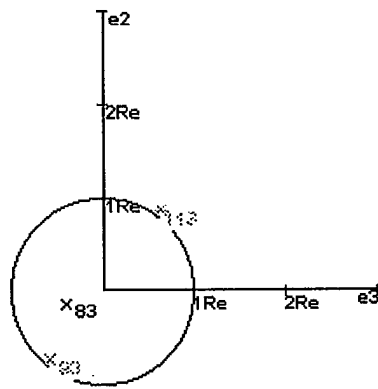
4.2.2 Trajectory 9. The impact conditions of trajectory 8 include an impact velocity of 68.6 km/sec, $\phi=120.0^\circ$, $\theta=115.0^\circ$.



Speed: 68.6 Phi: 120.0 Theta: 115.0 Detected 153.4 days out

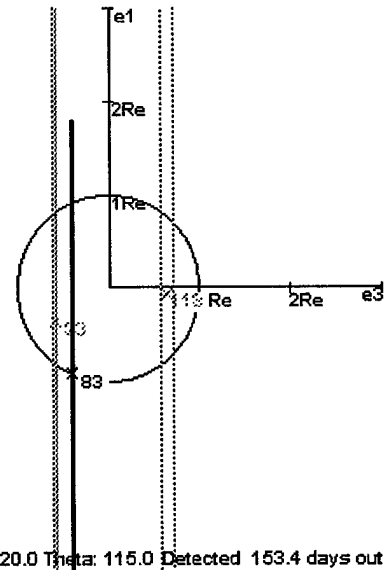
Figure 4.49. Trajectory 9 (Overhead View)

Trajectory 9, shown in Figure 4.49 is a retrograde trajectory that impacts the Earth after passing its point of perigee. This trajectory was selected to demonstrate sensitivity analysis in a different situation than trajectory 8. In fact, the velocity vector at impact is in the exact opposite direction of trajectory 8.



Speed: 68.6 Phi: 120.0 Theta: 115.0 Detected 153.4 days out

Figure 4.50. Error Ellipsoid (Velocity In, North Up)

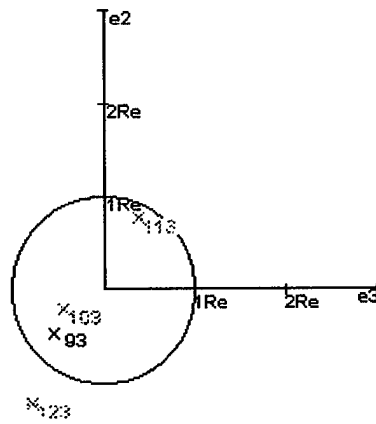


Speed: 68.6 Phi: 120.0 Theta: 115.0 Detected 153.4 days out

Figure 4.51. Error Ellipsoid (Velocity Up, North Out)

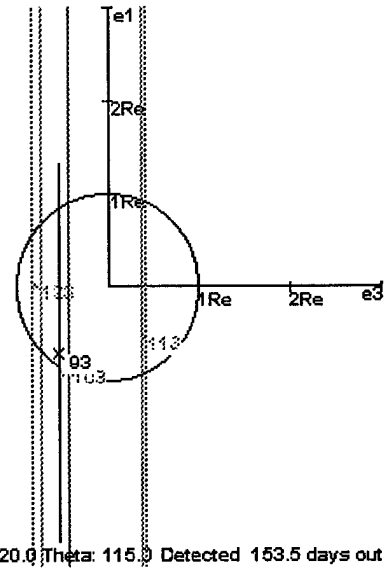
The error ellipsoids for this trajectory demonstrate that this trajectory rests in the moderate category concerning impact prediction. The NEO is detected 153 days out and a positive impact prediction occurs approximately 70 days later, leaving 83 days to react.

4.2.2.1 100 Observations Per Day.



Speed: 68.6 Phi: 120.0 Theta: 115.0 Detected 153.5 days out

Figure 4.52. Error Ellipsoid (Velocity In, North Up)

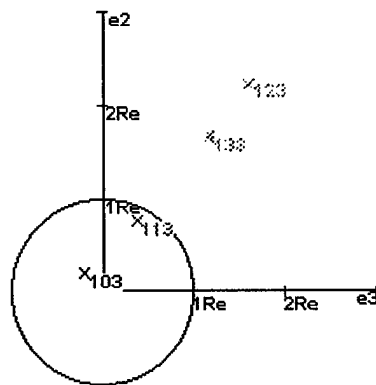


Speed: 68.6 Phi: 120.0 Theta: 115.0 Detected 153.5 days out

Figure 4.53. Error Ellipsoid (Velocity Up, North Out)

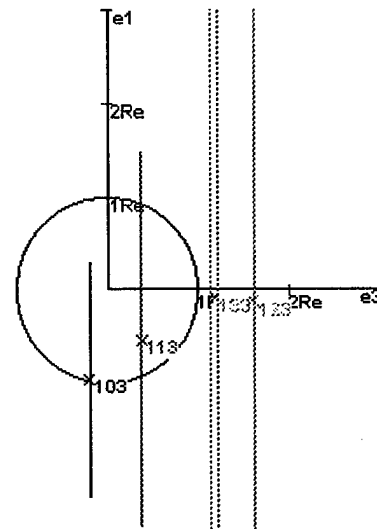
The result of increasing the number of observations to 100 per day is the same as with trajectory 8. The impact warning time grows by 10 days, a fairly significant improvement.

4.2.2.2 1000 Observations Per Day.



Speed: 68.6 Phi: 120.0 Theta: 115.0 Detected 153.3 days out

Figure 4.54. Error Ellipsoid (Velocity In, North Up)

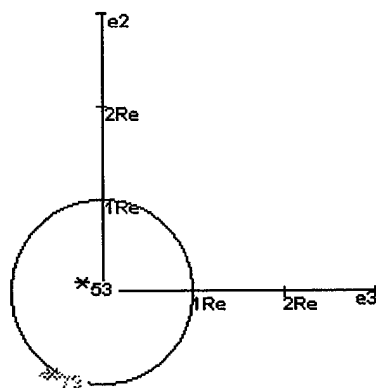


Speed: 68.6 Phi: 120.0 Theta: 115.0 Detected 153.3 days out

Figure 4.55. Error Ellipsoid (Velocity Up, North Out)

Once again, as illustrated in Figures 4.54 and 4.55, the results of increasing the number of observations per day to 1000 in turn increases the impact warning time by 20 days.

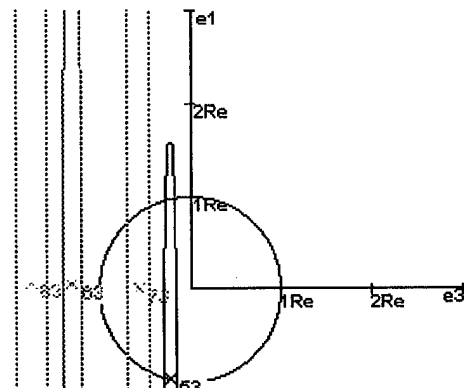
4.2.2.3 1.0 Arcsecond Accuracy.



*53

Speed: 68.6 $\frac{m}{s}$ 120.0 Theta: 115.0 Detected 153.4 days out

Figure 4.56. Error Ellipsoid (Velocity In, North Up)

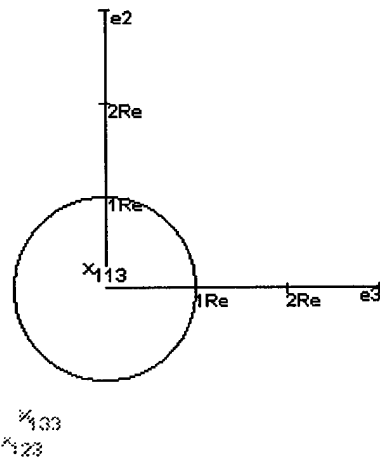


Speed: 68.6 $\frac{m}{s}$ 120.0 Theta: 115.0 Detected 153.4 days out

Figure 4.57. Error Ellipsoid (Velocity Up, North Out)

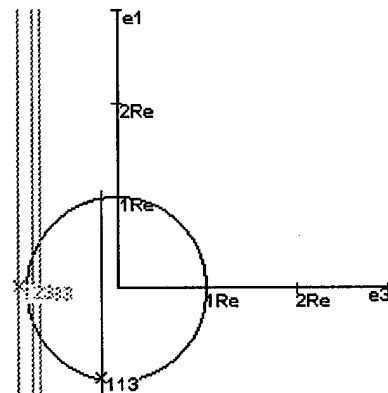
The results are again similar to the same analysis of trajectory 8. Decreasing the accuracy from 0.1 arcseconds to 1.0 arcseconds decreases the warning time by 30 days.

4.2.2.4 0.01 Arcsecond Accuracy.



Speed: 68.6 Phi: 120.0 Theta: 115.0 Detected 153.4 days out

Figure 4.58. Error Ellipsoid (Velocity In, North Up)

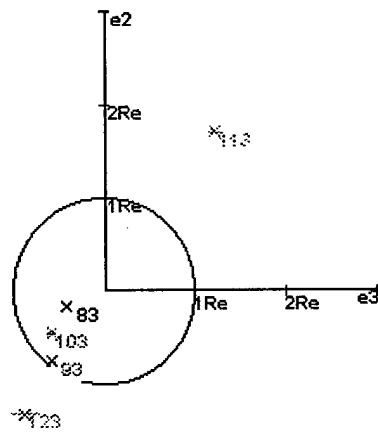


Speed: 68.6 Phi: 120.0 Theta: 115.0 Detected 153.4 days out

Figure 4.59. Error Ellipsoid (Velocity Up, North Out)

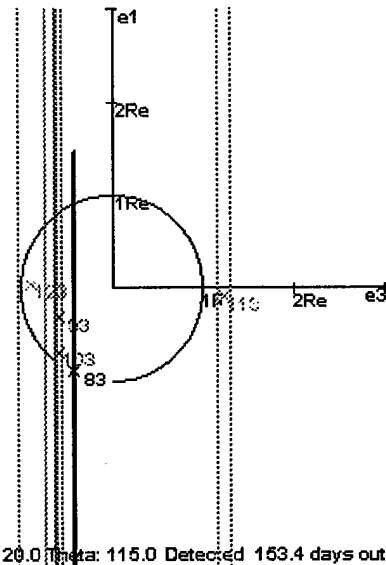
The resultant error ellipsoids for increasing the accuracy from 0.1 arcseconds to 0.01 arcseconds illustrate the first large deviation in regards to the sensitivity analysis of trajectories 8 and 9. For this case, the impact warning time increases by 30 days. Therefore, if the accuracy is increased by a factor of 10, the warning time increases by 30 days, and if the accuracy decreases by a factor of 10, the warning time decreases by 30 days.

4.2.2.5 Observations from the Moon.



Speed: 68.6 Phi: 120.0 Theta: 115.0 Detected 153.4 days out

Figure 4.60. Error Ellipsoid (Velocity In, North Up)

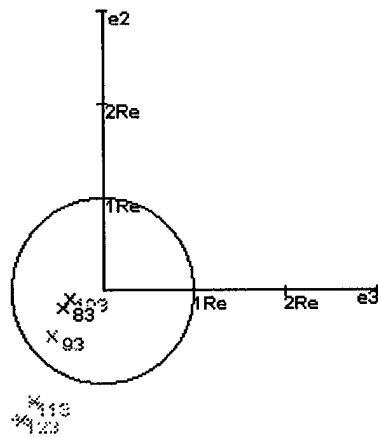


Speed: 68.6 Phi: 120.0 Theta: 115.0 Detected 153.4 days out

Figure 4.61. Error Ellipsoid (Velocity Up, North Out)

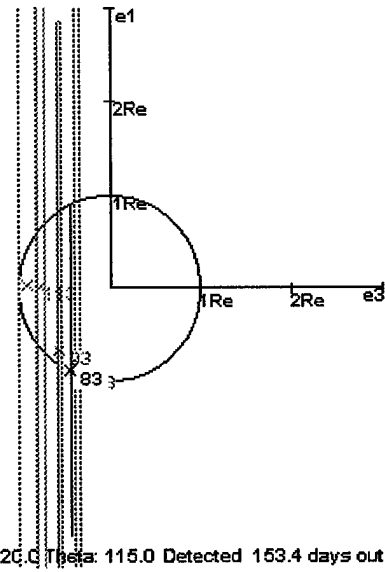
There is no significant increase in warning times associated with Moon oriented observational data.

4.2.2.6 Observations from Earth and the Moon.



Speed: 68.6 Phi: 120.0 Theta: 115.0 Detected 153.4 days out

Figure 4.62. Error Ellipsoid (Velocity In, North Up)

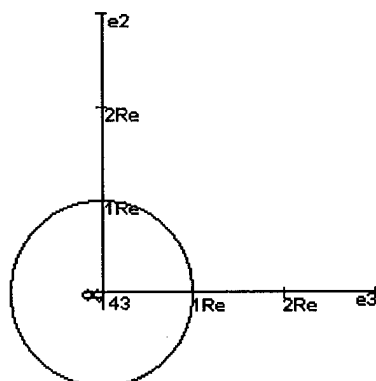


Speed: 68.6 Phi: 120.0 Theta: 115.0 Detected 153.4 days out

Figure 4.63. Error Ellipsoid (Velocity Up, North Out)

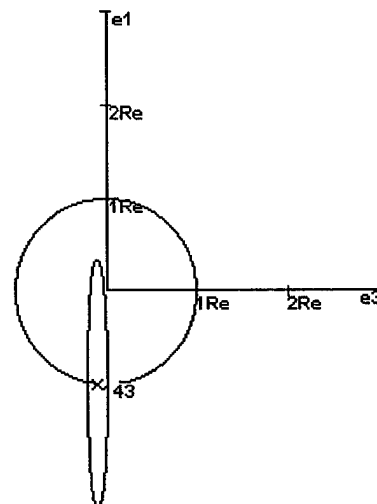
The error ellipsoids in Figures 4.62 and 4.63 illustrate that once again there is no significant improvement in impact accuracy by using this type of observational data. Although a slight decrease in the size of the final error ellipsoid at 83 days seems apparent, this is due to the fact that the number of data points created is slightly larger.

4.2.2.7 Observations from Earth and Mars.



Speed: 68.6 Phi: 120.0 Theta: 115.0 Detected 153.4 days out

Figure 4.64. Error Ellipsoid (Velocity In, North Up)

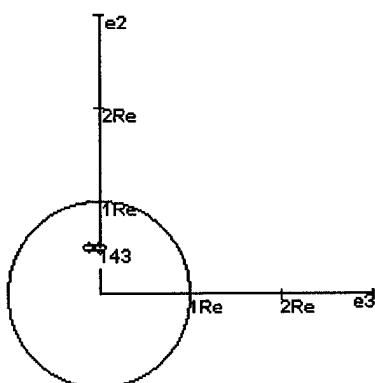


Speed: 68.6 Phi: 120.0 Theta: 115.0 Detected 153.4 days out

Figure 4.65. Error Ellipsoid (Velocity Up, North Out)

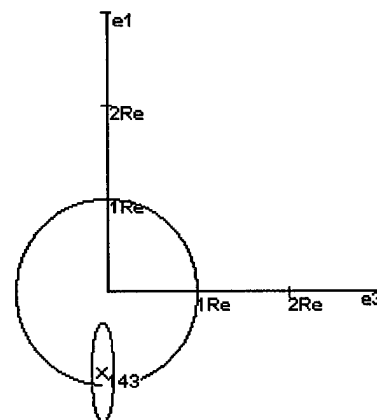
The large separation between Earth and Mars again results in successful triangulation, making the impact prediction easy. In this case it only takes 10 days of data to predict an impact. By analyzing the error ellipsoid, it is apparent that a larger error ellipsoid would positively predict an impact with this trajectory, so in all actuality, a positive impact prediction would probably take a couple days less.

4.2.2.8 Observations from Earth and an Out of Plane Orbit.



Speed: 68.6 Phi: 120.0 Theta: 115.0 Detected 153.4 days out

Figure 4.66. Error Ellipsoid (Velocity In, North Up)



Speed: 68.6 Phi: 120.0 Theta: 115.0 Detected 153.4 days out

Figure 4.67. Error Ellipsoid (Velocity Up, North Out)

Once again, the ensured large separation between the created observational satellite and the Earth provides data that is easily triangulated for a quick and accurate positive impact prediction.

4.2.3 Trajectory 1 (Revisited). In terms of NEO detection and impact prediction, this is the worst case scenario.

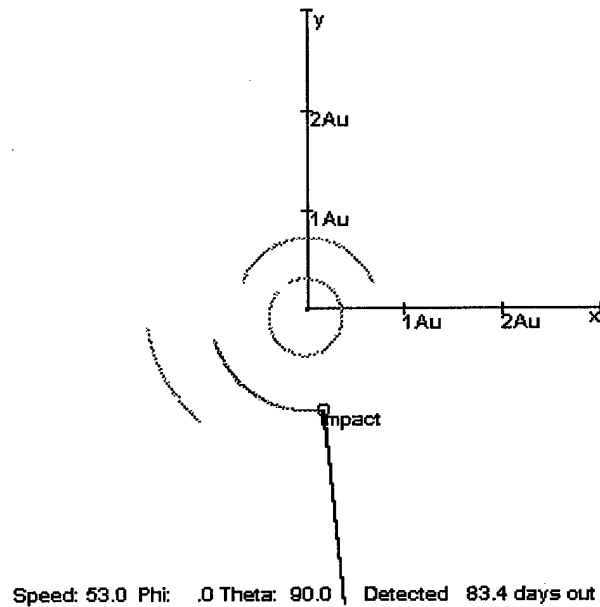


Figure 4.68. Trajectory 1 (Overhead View)

The trajectory in Figure 4.68 was briefly analyzed at the beginning of this section, however, it also is useful to demonstrate what can be done to improve the impact warning time.

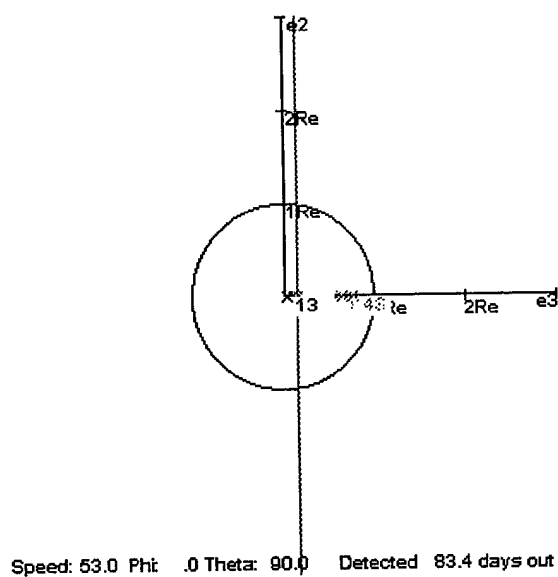


Figure 4.69. Error Ellipsoid (Velocity In, North Up)

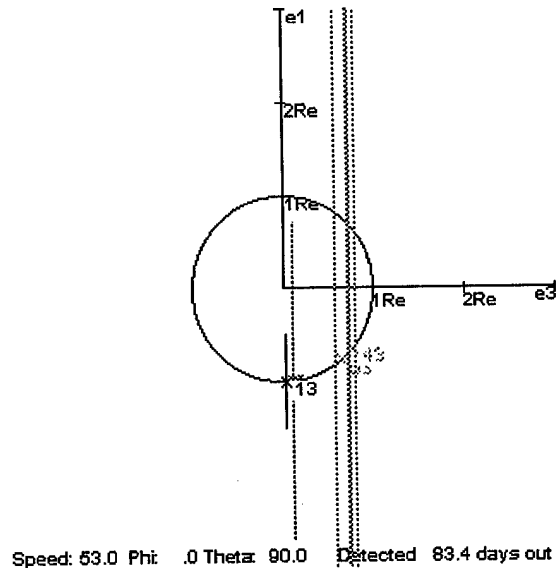
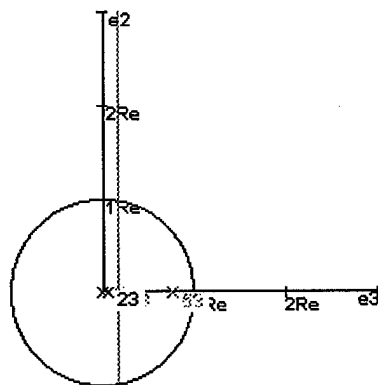


Figure 4.70. Error Ellipsoid (Velocity Up, North Out)

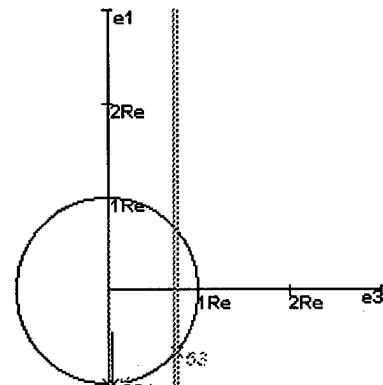
The original error ellipsoids are provided as a reference. Normal parameters lead to a positive impact prediction 13 days before impact.

4.2.3.1 100 Observations Per Day.



Speed: 53.0 Phi: .0 Theta: 90.0 Detected 83.4 days out

Figure 4.71. Error Ellipsoid (Velocity In, North Up)

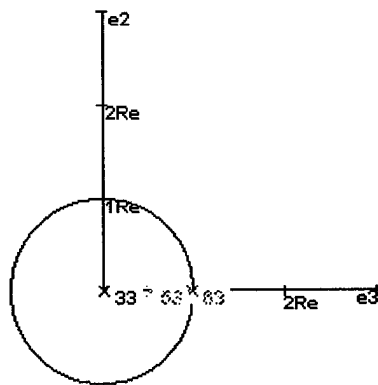


Speed: 53.0 Phi: .0 Theta: 90.0 Detected 83.4 days out

Figure 4.72. Error Ellipsoid (Velocity Up, North Out)

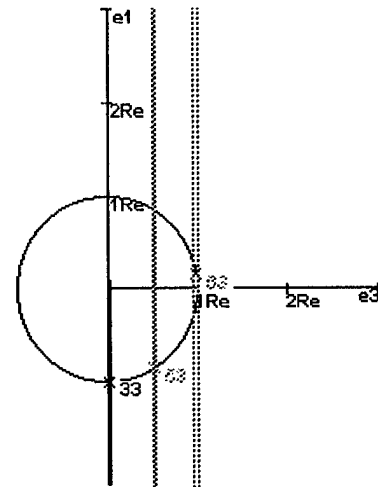
As with previous trajectories, increasing the number of observations per day by a factor of 10 improves the warning time by 10 days.

4.2.3.2 1000 Observations Per Day.



Speed: 53.0 Phi: .0 Theta: 90.0 Detected: 83.4 days out

Figure 4.73. Error Ellipsoid (Velocity In, North Up)

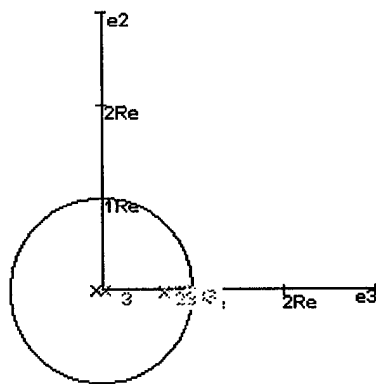


Speed: 53.0 Phi: .0 Theta: 90.0 Detected: 83.4 days out

Figure 4.74. Error Ellipsoid (Velocity Up, North Out)

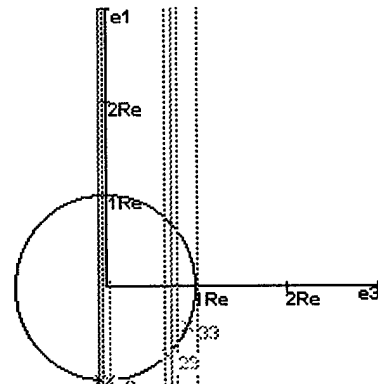
Increasing the number of observations taken per day from 10 to 1000 increases the warning time by 20 days. The results are the same as with trajectories 8 and 9.

4.2.3.3 1.0 Arcsecond Accuracy.



Speed: 53.0 Phi: .0 Theta: 90.0 Detected 83.4 days out

Figure 4.75. Error Ellipsoid (Velocity In, North Up)

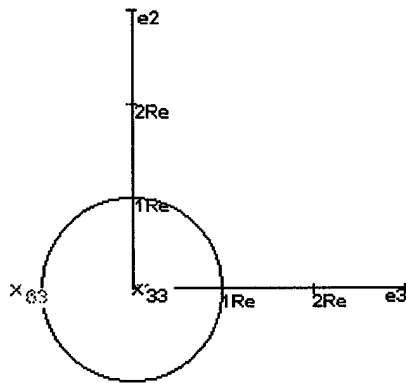


Speed: 53.0 Phi: .0 Theta: 90.0 Detected 83.4 days out

Figure 4.76. Error Ellipsoid (Velocity Up, North Out)

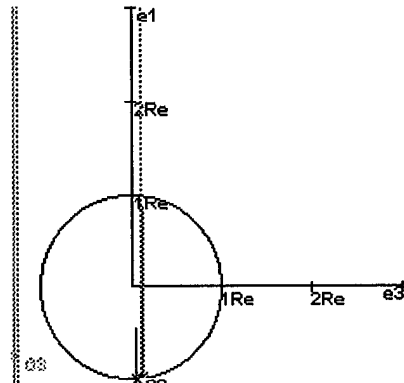
If the accuracy of the data is decreased by a factor of 10, the impact cannot be positively predicted even 3 days out. This is not acceptable.

4.2.3.4 0.01 Arcsecond Accuracy.



Speed: 53.0 Phi: .0 Theta: 90.0 Detected: 83.4 days out

Figure 4.77. Error Ellipsoid (Velocity In, North Up)

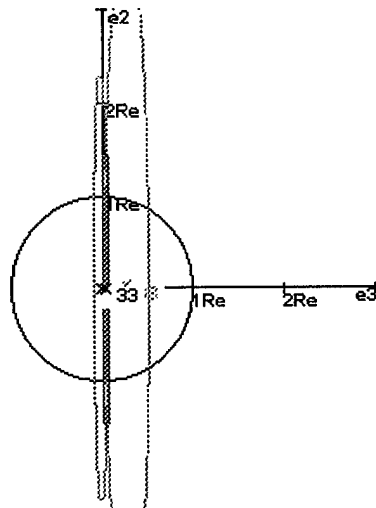


Speed: 53.0 Phi: .0 Theta: 90.0 Detected: 83.4 days out

Figure 4.78. Error Ellipsoid (Velocity Up, North Out)

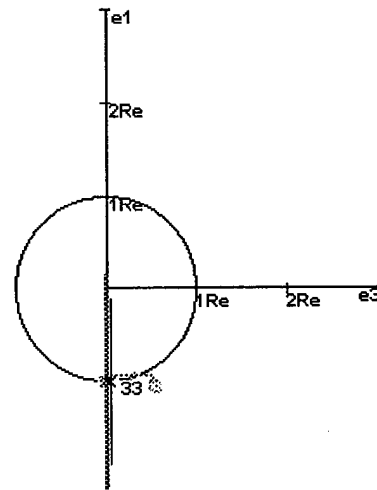
Figures 4.77 and 4.78 demonstrate that increasing the accuracy of the data by a factor of 10 increases the impact warning time by 20 days. This is a significant improvement if the accuracy can be accomplished.

4.2.3.5 Observations from the Moon.



Speed: 53.0 Phi: .0 Theta: 90.0 Detected 83.4 days out

Figure 4.79. Error Ellipsoid (Velocity In, North Up)



Speed: 53.0 Phi: .0 Theta: 90.0 Detected 83.4 days out

Figure 4.80. Error Ellipsoid (Velocity Up, North Out)

The error ellipsoids resulting from Moon originating observations demonstrate a large deviation from previous analysis of Moon centered observational data. For this trajectory, Moon observations improve the positive impact prediction time by 20 days. This is due to the fact that the closer an NEO is to the Earth, the easier it is to use sources close to the Earth to triangulate observations. Whereas at a distance of 10 AU, it takes observations from different planets to accomplish triangulation, close to the Earth, a satellite in a geosynchronous orbit could accomplish the same task.

4.2.3.6 Observations from Earth and the Moon.

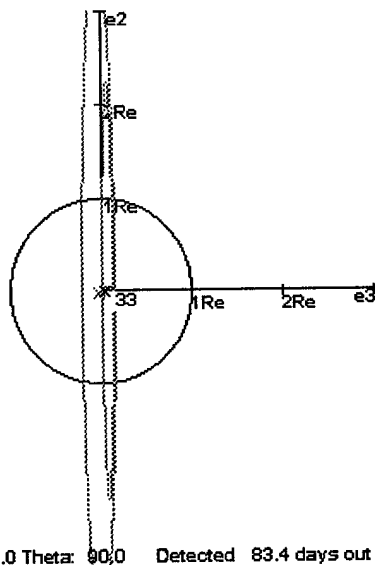


Figure 4.81. Error Ellipsoid (Velocity In, North Up)

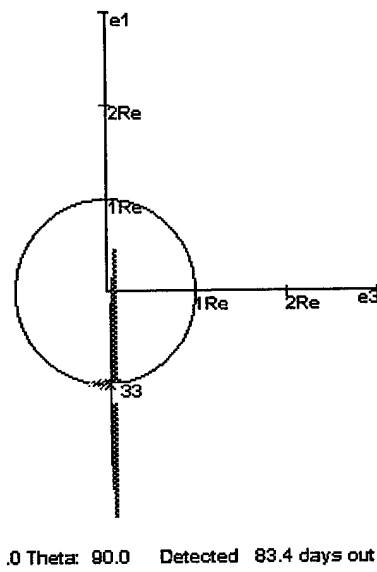
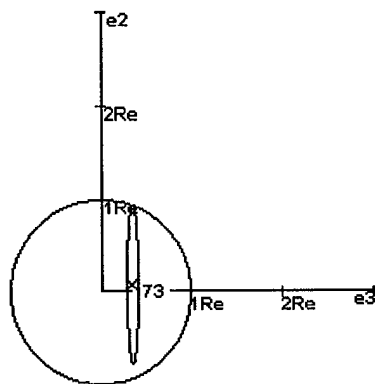


Figure 4.82. Error Ellipsoid (Velocity Up, North Out)

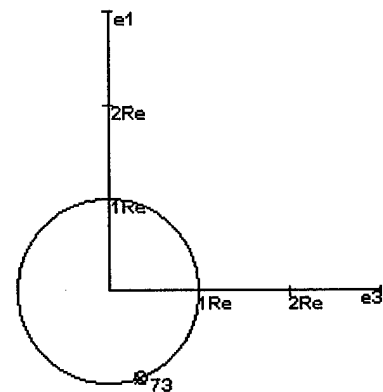
Using Earth and Moon data combined makes no significant impact warning time improvement over Moon data alone.

4.2.3.7 Observations from Earth and Mars.



Speed: 53.0 Phi: .0 Theta: 90.0 Detected 83.4 days out

Figure 4.83. Error Ellipsoid (Velocity In, North Up)

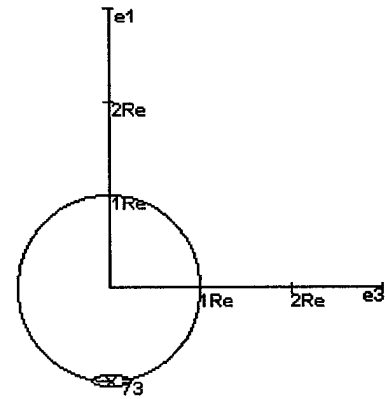
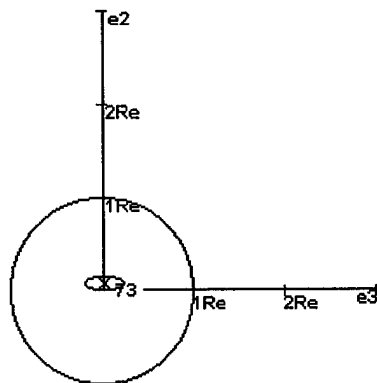


Speed: 53.0 Phi: .0 Theta: 90.0 Detected 83.4 days out

Figure 4.84. Error Ellipsoid (Velocity Up, North Out)

The impact warning time is vastly improved due to triangulation of sources that are relatively far apart.

4.2.3.8 Observations from Earth and an Out of Plane Orbit.



Speed: 53.0 Phi: .0 Theta: 90.0 Detected 83.4 days out

Speed: 53.0 Phi: .0 Theta: 90.0 Detected 83.4 days out

Figure 4.85. Error Ellipsoid (Velocity In, North Up)

Figure 4.86. Error Ellipsoid (Velocity Up, North Out)

As with trajectories 8 and 9, the out of Earth orbiting satellite provides accurate and immediate impact prediction.

V. Conclusions and Recommendations

5.1 Conclusions

On March 23, 1989, an asteroid bigger than an aircraft carrier, traveling at 46,000 miles per hour, passed through Earth's orbit less than 400,000 miles away. Our planet had been at that point only 6 hours earlier. The asteroid was not detected until after it had passed. Had it struck the Earth, the energy released would have been equivalent to that of 1000 to 2500 megatons of TNT. In an area of high population density such as the northeast corridor of the U.S., Los Angeles, or Tokyo, millions of people would have died instantly. (16:1)

There is no doubt that while remote, the threat of asteroid or comet impacts does exist. It is our choice on how and what we do to deal with it. The technology exists to enable us to detect and deflect the NEO before a possible cataclysmic event occurs.

While many specific trajectories and parameters were examined through the course of accomplishing this thesis, perhaps the most beneficial information exists in making large generalizations, which demonstrate difficulties and problem areas. In addition, the same generalizations can demonstrate the best ways to counter the problem areas and improve the impact prediction process.

With respect to NEO trajectories, several factors benefit impact predictions. The closer the inclination of an NEO's orbit is to 90° with respect to the Earth's orbit, the easier it is to predict a future impact using Earth centered observations. The further an object is out of the Earth's plane, the more the rotation of the Earth around the Sun will assist in the triangulation process. For the same reason, the more the observational source moves side to side with respect to the NEO, the easier it will be to predict a future impact. The closer an NEO passes to a large mass (i.e. the Sun or perhaps Mars) prior to

impact, the harder it is to predict a future impact. Tiny variations in the conditions before perigee will cause large differences in the impact predictions. The closer the NEO is to the observational source, the more accurate the data and impact predictions will be, for obvious reasons. The more time remains before impact, the more time there is to obtain more data and predict a possible future impact.

Technology also plays a large role in the ability to accurately predict a future impact. The type of observational data obtained by far outweighs any other factor when attempting to reduce the time taken to positively identify a future impact. Combining range data (radar or laser) with optical measurements provides the most beneficial data. The next most beneficial data source is provided by creating an observational satellite and placing it in an orbit 1 AU from the Sun, inclined 90° from the Earth's, and 180° out-of-phase with the Earth's orbit. The accuracy of the data, amazingly enough, has a large effect on the time it takes to predict impacts. Nothing below 0.1 arcseconds accuracy is acceptable for the purposes of Earth impact prediction. Finally, the more data that can be obtained, the better.

5.2 Recommendations

An endless number of variations of this thesis exist for future analysis and study. While this thesis only covered the extreme trajectories and two other randomly chosen trajectories, further study could investigate which trajectories should be given more focus from a real world operations standpoint. The number of observations made or resources allocated to particular NEOs could become a function of known models and could quickly vary as the NEOs trajectory becomes more familiar.

The following items may also deserve consideration for future studies:

- Take into account operational items including but not limited to obscurement of NEOs by weather and the Sun
- Alter the program to identify more precisely when the observational data leads to a positive impact prediction
- Create more observational sources, such as satellites located at the libration points
- Research more on existing technologies and efforts concerning long range radars and lasers for range determination

Bibliography

1. Allen, C., J. Archer, and P. Cerny. "Technology Application for an Earth Comet Asteroid Protection System," 1996 AIAA Space Programs and Technologies Conference. 1-7. Reston VA: American Institute of Aeronautics and Astronautics, Inc., 1996.
2. Archer, J., P. Cerny, and P. Odom. "System Architecture Concept for Earth Comet and Asteroid Protection," 1996 AIAA Space Programs and Technologies Conference. 1-7. Reston VA: American Institute of Aeronautics and Astronautics, Inc., 1996.
3. Bate, Roger R. and others. Fundamentals of Astrodynamics. New York: Dover Publications, Inc., 1971.
4. Bishop, Gregory Alan. Tracking and Impact Prediction of Earth-Crossing-Objects (ECOs) on a Collision Course with Earth. MS thesis. Wright-Patterson AFB OH, November 1994.
5. Bushman, A. V., and others. "Computer Simulation of Hypervelocity Impact and Asteroid Explosion," in Hazards Due to Comets and Asteroids. Ed. Tom Gehrels. Tucson: The University of Arizona Press, 1994.
6. Carusi, A. and others. "Near-Earth Objects: Present Search Programs," in Hazards Due to Comets and Asteroids. Ed. Tom Gehrels. Tucson: The University of Arizona Press, 1994.
7. Chapman, C. R. and others. "Physical Properties of the Near-Earth Asteroids: Implications for the Hazard Issue," in Hazards Due to Comets and Asteroids. Ed. Tom Gehrels. Tucson: The University of Arizona Press, 1994.
8. Friedman, G. "Risk Management of Planetary Defense," 1996 AIAA Space Programs and Technologies Conference. 1-14. Reston, VA: American Institute of Aeronautics and Astronautics, Inc., 1996.
9. Gehrels, Tom. "Collisions with Comets and Asteroids," Scientific American, 274: 54-59 (March 1996).
10. -----, "NEO Search Programs: Past, Present, and Future," 1996 AIAA Space Programs and Technologies Conference. 1-4. Reston VA: American Institute of Aeronautics and Astronautics, Inc., 1996.
11. Hogue, John. Nostradamus: The New Revelations. England: Element, 1 August 1995.

12. Lewis, John S. "Escaping the Ultimate Disaster-A Cosmic Collision," The Futurist, 31: 16-19 (January 1997).
13. Marsden, B. G. and D. I. Steel. "Warning Times and Impact Probabilities for Long-Period Comets," in Hazards Due to Comets and Asteroids. Ed. Tom Gehrels. Tucson: The University of Arizona Press, 1994.
14. Ostro, Steven J. "The Role of Groundbased Radar in Near-Earth Object Hazard Identification and Mitigation," in Hazards Due to Comets and Asteroids. Ed. Tom Gehrels. Tucson: The University of Arizona Press, 1994.
15. Remo, John L. "Classifying and Modeling NEO Material Properties and Interactions," in Hazards Due to Comets and Asteroids. Ed. Tom Gehrels. Tucson: The University of Arizona Press, 1994.
16. Tagliaferri, E. "The History of AIAA's Interest in Planetary Defense," 1996 AIAA Space Programs and Technologies Conference. 1-4. Reston VA: American Institute of Aeronautics and Astronautics, Inc., 1996.
17. Wiesel, Dr. William E. Bayes Filter/ FORTRAN Library Units. School of Engineering, Air Force Institute of Technology, Wright-Patterson AFB OH, April 1997.
18. -----. Class text for MECH 636, Advanced Astrodynamics. School of Engineering, Air Force Institute of Technology, Wright-Patterson AFB OH, January 1997.
19. -----. Class text for MECH 731, Advanced Astrodynamics. School of Engineering, Air Force Institute of Technology, Wright-Patterson AFB OH, April 1997.

VITA

Captain Ahren D. Heidt was born on 31 October 1970 in Raleigh, North Carolina. He lived briefly in California, then moved to Boise, Idaho in 1973 where he graduated from Capital High School in 1989. Upon graduation, he entered the United States Air Force Academy. He graduated with a Bachelor of Science Degree in Space Physics and was commissioned a Second Lieutenant in June 1993. Following graduation, he received a temporary assignment at the United States Air Force Academy in the Electrical Engineering Department. He completed Undergraduate Space Training in January 1994, and was assigned to the 2nd Space Warning Squadron, Buckley ANG Base, Colorado.

Captain Heidt completed the Commander's Course at the 21st Crew Training Squadron in June 1994. He was then assigned to 2SWS as a Crew Commander until June 95 when he served as Assistant Chief, Standardization and Evaluation. Additionally, he has served as both line instructor and line evaluator during his tour at 2SWS.

Captain Heidt is currently attending the Air Force Institute of Technology in pursuit of a Master's Degree in Space Operations. Capt Heidt is married to the former Nicole Marie Wenke of Casper, Wyoming. They have two sons, Kaleb and Jadon.

Permanent Address: 2557 Bruins Circle
Boise ID 83704

REPORT DOCUMENTATION PAGE			Form Approved OMB No. 0704-0188	
Public reporting burden for this collection of information is estimated to average 1 hour per response, including the time for reviewing instructions, searching existing data sources, gathering and maintaining the data needed, and completing and reviewing the collection of information. Send comments regarding this burden estimate or any other aspect of this collection of information, including suggestions for reducing this burden, to Washington Headquarters Services, Directorate for Information Operations and Reports, 1215 Jefferson Davis Highway, Suite 1204, Arlington, VA 22202-4302, and to the Office of Management and Budget, Paperwork Reduction Project (0704-0188), Washington, DC 20503.				
1. AGENCY USE ONLY (Leave blank)		2. REPORT DATE December 97		3. REPORT TYPE AND DATES COVERED Master's Thesis
4. TITLE AND SUBTITLE WARNING TIMES AND IMPACT PREDICTIONS OF ASTEROIDS AND COMETS ON A COLLISION COURSE WITH EARTH			5. FUNDING NUMBERS	
6. AUTHOR(S) Ahren D. Heidt, Captain, USAF				
7. PERFORMING ORGANIZATION NAME(S) AND ADDRESS(ES) Air Force Institute of Technology 2750 P Street WPAFB OH 45433-7765			8. PERFORMING ORGANIZATION REPORT NUMBER AFIT/GSO/ENY/97D-1	
9. SPONSORING/MONITORING AGENCY NAME(S) AND ADDRESS(ES) Salvatore Alfaro, Colonel, USAF HQ US Space Cmd/AN 250 S Peterson Blvd, Suite 116 Peterson AFB CO 80914-3180			10. SPONSORING/MONITORING AGENCY REPORT NUMBER	
11. SUPPLEMENTARY NOTES				
12a. DISTRIBUTION AVAILABILITY STATEMENT Approved for public release; distribution unlimited.			12b. DISTRIBUTION CODE	
13. ABSTRACT (Maximum 200 words) <p>This study investigates the amount of data and time necessary to accurately predict Earth impacts of Earth-Crossing-Objects (ECOs). Trajectories are simulated by numerically integrating in an N-Body system. Given final impact parameters, the trajectory is propagated backwards to an earlier time, creating initial conditions and simulated observation data at requested intervals to which Gaussian random noise is introduced. Utilizing a Bayes Filter to estimate position and velocity from the simulated observation data, the estimate is then propagated forward in time to determine whether or not an impact can be accurately predicted. State vectors and covariance matrices are then propagated to the impact time and the one-sigma error ellipsoid is analyzed.</p>				
14. SUBJECT TERMS Asteroids, Collisions, Comets, Earth, Impact Prediction			15. NUMBER OF PAGES 101	
			16. PRICE CODE	
17. SECURITY CLASSIFICATION OF REPORT UNCLASSIFIED	18. SECURITY CLASSIFICATION OF THIS PAGE UNCLASSIFIED	19. SECURITY CLASSIFICATION OF ABSTRACT UNCLASSIFIED	20. LIMITATION OF ABSTRACT UL	